

## The Effect of Moisture on the Diffusion of Organic Molecules in Coal

Yoshinobu Otake and Eric M. Suuberg  
Division of Engineering  
Brown University  
Providence, R.I. 02912

### INTRODUCTION

Diffusional limitations are of importance in a large number of coal utilization processes. Common examples may be seen in many different kinds of processes; in donor solvent liquefaction, the coal must be broken down finely enough so that donor solvent transport into the coal does not become a limiting step (this is generally true at the usual process conditions); in coal devolatilization, during a pyrolysis or combustion process, the rate of escape of tars from coal particles is often limited by diffusional mass transfer in the particles; in natural weathering of coal, diffusional processes limit the rate of oxidation. The potential list of examples is much longer, and it may be quickly concluded that from a technological point of view, knowledge of diffusion rates in coals is generally quite useful. Relatively little such information exists in the literature because the historical method of handling questions of diffusional limitations has involved the empirical approach of grinding particles progressively finer, until no effects of further comminution were seen in the chemistry of interest. As the understanding of the chemical mechanisms involved in coal processing has improved, it now makes sense to improve on the understanding of the transport phenomena as well, and to move away from the empirical approaches to handling questions concerning mass transfer.

The present paper is concerned with diffusional transport occurring in both 1. micropores, and 2. the bulk solid. The distinction between processes in these two nominally distinct places in the coal is unimportant, because the distinction between "micropores" and "gaps between molecules" in a bulk solid is not always clear. The well-known problem of measuring surface areas of coals with  $N_2$  and  $CO_2$  is an example. There are certain portions of the coal porosity that are inaccessible to  $N_2$  that are quite accessible to  $CO_2$ , despite the fact that the latter is a larger molecule than the former. This is because diffusion on the micropore level is activated, meaning that thermal motion of the coal structure is required in order for the gas molecules to be able to penetrate the gaps between the molecules.  $N_2$  is apparently less able to penetrate the structure than  $CO_2$  because the experiments with  $N_2$  must normally be performed at very low temperatures (i.e. liquid nitrogen temperatures), and the magnitude of the vibrations in the coal structure are not large enough at this temperature to open up sufficiently large gaps for large amounts of  $N_2$  to penetrate. The magnitude of motions required for penetration by molecules depends upon the size of the penetrant species, and the nature of interactions between the coal and the species. Thus what may appear to be impenetrable bulk solid to one molecule may appear to be porosity to another.

It is the process of activated diffusion in coals that is of principal interest in this paper. There have been a limited number of other earlier studies of activated diffusion processes in coals, particularly concerning the diffusion of small gas molecules (e.g.  $CH_4$ ,  $CO_2$ , light hydrocarbons, noble gases), through bulk coals. This study is, however, mainly concerned with the activated diffusion of larger organic species in coals. In the present case, common "swelling solvents" such as water, pyridine, tetrahydrofuran (THF) are of interest. These are termed swelling solvents because when a dried coal sample is immersed in them, it will physically swell as the solvents are imbedded. The theory of solvent swelling in coals has been well described elsewhere<sup>1</sup>, and is based on the classic technique as developed for characterization of crosslinked polymers<sup>2</sup>. The simplest relationship that embodies the essence of the technique is the Flory-Rehner equation, a relationship between the molecular weight between crosslinks in a polymer (M) and the extent to which the polymer is volumetrically swollen by a particular solvent (Q):

$$M = \left[ \frac{\rho_c M_s}{\rho_s} \right] \left[ \frac{(1/2Q) - (1/Q)^{1/3}}{\ln [1 - (1/Q)] + (1/Q) + \chi(1/Q)^2} \right]$$

where  $\rho_c$  is the density of the original coal,  $\rho_s$  is the density of the solvent,  $M_s$  is the molecular weight of the solvent and  $\chi$  is the solvent-network interaction parameter. The measurement of  $\chi$  is difficult, as is its estimation for specifically interacting solvents such as pyridine. Values range between 0.3 and 0.6 for typical pairs of solvents and coals. It has been suggested that the Flory-Rehner equation does not hold particularly well for coals, which are highly crosslinked rigid networks<sup>3,4</sup>. Its use here is only illustrative, and more sophisticated approaches have been developed<sup>5-6</sup>; unfortunately these new models require more information about the structure of the coal-- namely, the molecular weight of repeat units within the coal structure. Since such information is not readily available at present, this will tend to restrict somewhat the use of these more realistic models.

The nature of the combined diffusion and solvent swelling process has also received attention in the literature in recent years<sup>7-9</sup>. This process, observed in "good" solvents-- those that swell the coal structure significantly -- is often non-Fickian in nature. Instead, it is often controlled by what is termed as relaxation of the coal macromolecules, and the process is characterized as exhibiting "Case-II" diffusional behavior. This behavior is well known in polymer systems that are below their glass transition temperatures. It is normally identified by noting that the rate of solvent uptake, or alternatively polymer swelling, is proportional to time, rather than square root of time as in Fickian processes.

What has received relatively little attention thus far in the literature on this topic is the activation energy for the combined diffusion and swelling process. This activation energy will depend upon the nature of the relaxation process that occurs in the glassy coal structure. Below its decomposition temperature, an unswollen coal is below its glass transition temperature<sup>1</sup>, but solvent imbibition lowers the glass transition temperature significantly<sup>10</sup>. For the temperatures of interest in this study, the coal will always initially be in the glassy regime.

It is likely that the diffusion rate of a swelling solvent in a glassy material (coal) will be significantly altered by the presence of another swelling solvent. The swelling of coals in mixed solvents has been previously studied in binary mixtures, and co-operative effects noted<sup>11</sup>. But a special case of this effect might involve diffusion in coals that are undried or incompletely dried. In such a case, the water present in the coal may influence the diffusion process, by virtue of being a swelling solvent itself. The swelling and shrinkage behavior of lignites with respect to moisture gain and loss has been reported on in some detail<sup>12,13</sup>, and other recent results suggest that even bituminous coals behave similarly, as colloidal materials, with respect to water as a solvent<sup>14</sup>. In the present study, the effect of moisture content on the diffusion behavior of solvents, in various ranks of coal, is considered.

## EXPERIMENTAL

The analyses of the coals examined in this study are provided in Table 1. Except where otherwise noted, the coals were ground and sieved to the size range 53-88 $\mu$ m. Special care was given to the lignites to avoid any more drying than necessary while processing. The first four samples in Table 1 were judged to have dried to only a limited extent since mining, and all were crushed in-house from large lumps. To prevent drying, these four samples were stored at 100% relative humidity conditions, at room temperature, by suspending the samples above a large reservoir of clean water, in a sealed container. It is of course difficult in practice to maintain truly 100% relative humidity conditions in such a manner, particularly if the chamber must be occasionally opened for sample removal. There was consequently a small difference in measured moisture contents between bed-moist samples (which are effectively immersed storage samples) and those used in this study. The difficulty in characterizing the initial moisture contents of immersed samples was what prompted us to use this slightly different storage method. Related sample storage and characterization information concerning these lignites can be found elsewhere<sup>13</sup>.

The principal experimental technique employed throughout this study was solvent swelling. The technique involves immersion of prepared, sized, coal samples in pure solvents. The measurements were performed in tubes of only a few millimeters inner diameter, and less than 5 cm in length. This technique permitted such measurements to be made with modest quantities of sample. The sample and solvent is frequently stirred during the first phases of the swelling process to prevent plugging in the bottom of the tubes. The tubes are immediately immersed in thermostatted water baths, after mixing coal and solvent. The small diameter of the tubes and the frequent stirring of their contents assure isothermality in the tubes, a necessary prerequisite for obtaining good rate data.

Rate data for swelling are obtained from measurements of the height of the column of coal as a function of time. Since the tubes are of uniform cross-section, the height change of the column of coal is proportional to the volume change in the sample. It is necessary to centrifuge the column of coal in order to obtain reliable measurements. The initial height is obtained by centrifuging the dry sample. Subsequent readings are obtained by first quenching the sample in an ice bath (if necessary because of rapid swelling kinetics) and then centrifuging the partially swollen coal sample for about ten minutes before taking readings. For this purpose, a high speed centrifuge with internal cooling has proven useful.

Thus the raw data of this study are swelling ratios as a function of time, temperature, solvent and coal. Standard Arrhenius plots of log of the swelling rate vs. inverse temperature provide the activation energies for the diffusion/swelling processes.

## RESULTS AND DISCUSSION

It has recently been reported that a wide range of coal ranks seem to obey a common relationship between moisture loss and volumetric shrinkage<sup>14</sup>. A correlation was developed for the set of coals shown in Table 1:

$$\% \text{ Volumetric Shrinkage} = 0.94 (\text{Moisture Loss, wt } \%) - 0.6$$

It was noted that even high volatile bituminous coals, with only a percent or two moisture content, follow this correlation. It is interesting to note that the bituminous coals that show such weakly swelling gel behavior with water as a solvent may typically swell to double their original volume in pyridine. The lignites swell to about 30% extent in water, and also can roughly double their volume in pyridine. The reason for this difference in behaviors is not fully understood. It is obvious that lignites possess much higher amounts of surface oxygen functional groups than do bituminous coals. This would suggest that the value of  $\chi$  in the Flory-Rehner equation is higher for lignite-water interactions than for bituminous coal-water interactions. But the differences in water swelling behavior may only be partly based on differences in  $\chi$  values. Another possible explanation is that the apparent molecular weight ( $M$ ) between crosslinks in bituminous coals is lower than in lignites, because water is unable to disrupt some kind of non-covalent crosslinking interactions that pyridine is able to disrupt (e.g. interactions between neighboring aromatic clusters). Which of these effects is predominant is, at present, not clear, and indeed both may play some role.

The effect that moisture content in coals may have on diffusion rates of other solvents in the coals is illustrated in Figures 1 and 2, in which the rate of swelling in pyridine is compared for both "wet" and "dry" coal samples. The data in Figure 1 show the 25°C pyridine swelling behavior of the dry and partially moist Texas lignite samples (particle size 212-300 $\mu$ m). The top panel shows the actual raw data, and the lower panel shows the same data, with a correction applied to the data for the moist lignite. The moist lignite has already been partially swollen by water, and in order to compare the data for the moist lignite with those for the dried lignite, it is necessary to express them on a common dry lignite basis. This has been accomplished in the bottom part of Fig. 1 by multiplying the actual swelling ratio (relative to the moist lignite volume) by the swelling ratio observed in going from a dry state to a 9% moisture condition. It is apparent that after such a correction, the final equilibrium swelling ratios in pyridine are identical for the two samples.

The rate of swelling in the case of the wet lignite is, however, considerably higher than the rate of swelling

of the dried lignite. Similar behavior has been noted in the swelling behavior of dried and wet lignites in THF; the swelling of a wet sample is faster than that of a dried sample.

Figure 2 shows that the same conclusion may be drawn in the case of the Powhatan #5 bituminous coal. The particle size range (212-300 $\mu$ m) and temperature (25 $^{\circ}$ C) were identical to those employed in the case of the lignite tests. The presence of moisture accelerates the rate of swelling of the coal by other solvents. Note, however, from the very different timescales in Figs. 1 and 2 that the diffusion and swelling processes in the two coals must be quite different. The swelling rate in the case of the bituminous coal is much higher than that in the lignite. This is consistent with earlier results on the diffusion of pyridine in dried bituminous coals and lignites, in which the activation energy for diffusion/swelling in several bituminous coals was about 13 kcal/mol, and in another lignite it was 18 kcal/mol<sup>14</sup>. Thus it seems in some sense easier for the pyridine to diffuse in and swell the bituminous coal than the lignite. The reasons for this are not yet understood. The effect does not, however, appear related to the presence or absence of moisture in the coals, since the timescale difference exists for both wet and dried samples. In fact, the difference in the rates of the diffusion and swelling processes appears to be a characteristic of the structure of the coals, since, the timescale for THF swelling of the Texas lignite is comparable to that for pyridine swelling of the lignite. Thus, one may conclude that the swelling processes are inherently slower in lignites than in bituminous coals, but that they are affected in the same way by moisture in both cases.

There may be concern that the apparent effect of moisture content on diffusion rates is an artifact, due to some kind of irreversible collapse of the structure upon drying. This was proven to not be the case in an experiment in which samples of the Beulah lignite were dried at vacuum for 3 hours, at 100 $^{\circ}$ C, and then allowed to regain varying amounts of moisture, by exposure to different relative humidity environments. The samples were then subjected to pyridine swelling at 35 $^{\circ}$ C. The effect of moisture content was as noted previously in the case of the Texas lignite. Figure 3 presents a summary of results. The curves show the times required for the samples to reach 30 and 50% of their final extents of swelling (relative to the particular initial volumes of each sample). The conclusion is that the more swollen the coal is to start with, the less time is required to reach any additional extent of swelling.

Indicated for each data point in Figure 3 are the activation energies for pyridine swelling, calculated for each sample at a constant extent of swelling, i.e. either 30% or 50%. These were determined for the range of temperatures 25 $^{\circ}$ C to 58 $^{\circ}$ C. It is interesting to note that while additional moisture appears to accelerate the rate of swelling in pyridine, the presence of moisture also seems to increase the activation energy for additional swelling.

It has been noted in the polymer literature that the higher the glass transition temperature a polymer exhibits, the lower the activation for ordinary diffusion of light gas molecules in that polymer<sup>15</sup>. While the combined swelling and diffusion process in coals is considerably more complex than the diffusion of light gases in polymers, the trends may indeed be related. In Figure 3 it is observed that the activation energy for swelling and diffusion is highest in the highest water content samples. It is well known that the addition of a swelling solvent to a glassy structure will lower its glass transition temperature, and thus the moister the coal, the lower its glass transition temperature. The data are thus in qualitative agreement with trends observed in the polymer literature.

To explore more fully the question of effect of crosslinking and reduced mobility of the coal structure on the rate of diffusion of pyridine in coals, a separate set of experiments was performed at various sets of heat treatment conditions. It has been shown previously that heat treatment of lignites at temperatures in the range 100 $^{\circ}$ C to 300 $^{\circ}$ C results in significant irreversible changes in the structure of the materials, both in terms of collapse of porosity and crosslinking of the structure<sup>15,14</sup>. Based on the trends reported above, one would expect that increasing the severity of heat treatment would lead to increasing crosslinking of the structure, and thus to decreasing activation energy for the swelling and diffusion process. (This is because increased crosslinking in highly crosslinked materials will lead to further increases in the glass transition temperature). The results in Table 2 confirm this hypothesis, and thus lend support to the view that the role of

water in raising the activation energy for the diffusion process is merely in decreasing the glassy character of the coal.

The above observations of decreased activation energy for diffusion and swelling of the coals or polymers, with increased rigidity of the structure (due to crosslinking) might be initially counterintuitive. But it should be noted that the more highly crosslinked and rigid the network structure, the more the activation energy is concentrated in a smaller number of degrees of freedom, in the area in which the activated process is occurring<sup>16</sup>. Thus an increase in activation energy with increased extent of preswelling is likely to be reflecting the fact that there is progressively more mobility in the coal macromolecule, the more it is swollen. Hand-in-hand with increased mobility is the requirement for greater thermal energy to access progressively less probable configurations, which will allow for further swelling. To keep this physical picture in perspective, it should be recalled that the individual "chains" in the coal macromolecule are probably behaving mainly as "entropy springs"- the free energy change associated with swelling, or stretching the chains in the coal macromolecule is positive, due to entropic losses. The negative free energy change that balances this positive free energy change, in the Flory-Rehner analysis, arises from the decrease in chemical potential of the solvent, as it interacts with the structure. The activation energy of the process reflects the need to assume the progressively less probable chain configurations, via thermal motions of the chain segments, as the structure swells.

## CONCLUSIONS

The results of the present study confirm the importance of establishing and reporting carefully the moisture content of any coal that is the subject of diffusion rate and/or swelling rate measurements. Likewise, it is important to report carefully how a sample may have been dried, prior to these measurements, since such low temperature procedures also may influence the results.

It may be concluded from the present work that moisture will swell coals of bituminous, subbituminous, and lignite ranks. This swelling will permit faster penetration and swelling of the coal structure by organic liquid diffusants. The activation energies observed for such swelling processes are reduced, as the effective glass transition temperature of the coals are increased, either by drying or pyrolysis.

## ACKNOWLEDGEMENT

The support of the USDOE through grants DE-FG22-85PC80527 and DE-AC18-84FC10617, and the Exxon Education Foundation, is gratefully acknowledged.

## REFERENCES

1. Green, T., Kovac, J., Brenner, D., and Larsen, J.W., in Coal Structure, R. Meyers, Ed., Chapter 6, Academic Press, 1982.
2. Flory, P.J. and Rehner, J. J. Chem. Phys. **11**, 521 (1943).
3. Larsen, J.W. and Kovac, J., ACS Symp. Ser. No. 71, 36 (1978).
4. Lucht, L.M. and Peppas, N.A. ACS Symp. Ser. No. 169, 43 (1981).
5. Kovac, J., Macromolecules, **11**, 362 (1978).
6. Peppas, N., Lucht, L., Hill-Lievensen, M., Hooker, A., DOE Final Tech. Report DE-FG22-80PC3022, US Dept. of Energy, 1983.
7. Ritger, P.L. and Peppas, N.A., Fuel, **66**, 815 and 1379 (1987) and references therein.
8. Hsieh, S.T. and Duda, J.L., Fuel, **66**, 170 (1987).
9. Brenner, D. and Hagan, P.S., ACS Div. Fuel Chem. Prepr., **30(1)**, 71 and 83 (1985).
10. Lucht, L.M., Larson, J.M., and Peppas, N.A., Energy & Fuels, **1**, 56 (1987).
11. Green, T.K. and Larsen, J.W., Fuel, **63**, 1538 (1984).
12. Evans, D.G., Fuel, **52**, 186 (1973).
13. Deevi, S. and Suuberg, E.M., Fuel, **66**, 454 (1987).
14. Suuberg, E.M., Otake, Y. and Deevi, S., ACS Div. Fuel Chem. Prepr., **33(1)**, 387 (1988).
15. Van Krevelen, D.W., Properties of Polymers (2nd Edition), Chapter 18, Elsevier, 1976.
16. Rogers, C.E., in Polymer Permeability, J. Comyn, Ed., Chapter 1, Elsevier, 1985.

Table 1-Coals Studied

<u>sSAMPLE</u>	<u>C</u>	<u>H</u>	<u>N</u>	<u>S</u>	<u>ASH</u>	<u>O</u>	<u>Moisture</u>
Beulah lignite <sup>a</sup>	65.6	3.6	1.1	0.8	11.0	17.9	26.0
Freedom lignite <sup>a</sup>	63.5	3.8	0.9	1.4	6.1	24.3	27.9
Glenn Harold lignite <sup>a</sup>	61.1	4.4	0.8	0.4	7.4	25.9	28.9
Gascoyne lignite <sup>a</sup>	60.9	4.2	0.6	1.4	8.2	24.7	30.7
Beulah lignite <sup>b</sup>	65.9	4.4	1.0	0.8	9.7	18.2	32.2
Texas lignite (PSOC1036) <sup>c</sup>	61.5	4.7	1.4	1.3	12.5	18.5	31.8
Belle Ayr Subbit.	69.3	4.4	1.0	0.5	10.3	14.5	30.3
Big Brown Subbit.(PSOC785) <sup>c</sup>	62.8	4.6	1.1	1.1	12.6	17.8	27.8
Montana Subbit.(PSOC837) <sup>c</sup>	57.8	4.3	0.8	0.7	11.9	24.6	17.0
Pittsburgh No.8 (HVBit.) <sup>b</sup>	74.2	4.1	1.4	2.3	13.2	4.8	1.7
Bruceton HVBit. <sup>d</sup>	80.4	5.3	1.6	1.0	4.6	6.7	1.7
Powhatan HVBit.	72.3	5.1	1.5	3.6	9.7	7.8	1.1

•All results on a dry weight percent basis, except moisture which is ASTM value on an as-received, bed moist basis.

•Oxygen by difference.

a- Grand Forks Energy Research Center lignite sample bank.

b- Argonne National Laboratory Premium Coal Samples.

c- Pennsylvania State University Coal Sample Bank.

d- U.S. Bureau of Mines Standard Sample.

Table 2- Effect of Drying Temperature on the Activation Energy for Pyridine Diffusion/Swelling Processes in Beulah Lignite

<u>Drying Temperature (°C)</u>	<u>Q(equilibrium)</u>	<u>Activation Energy (kcal/mol)</u>
100	1.86	17.7
200	1.78	16.5
320	1.70	13.9

•All samples were predried in vacuum for 3 hours, and then subsequently dried at the indicated temperatures for 1 hour additional, under nitrogen.

•All swelling ratios determined in pyridine, at 35°C.

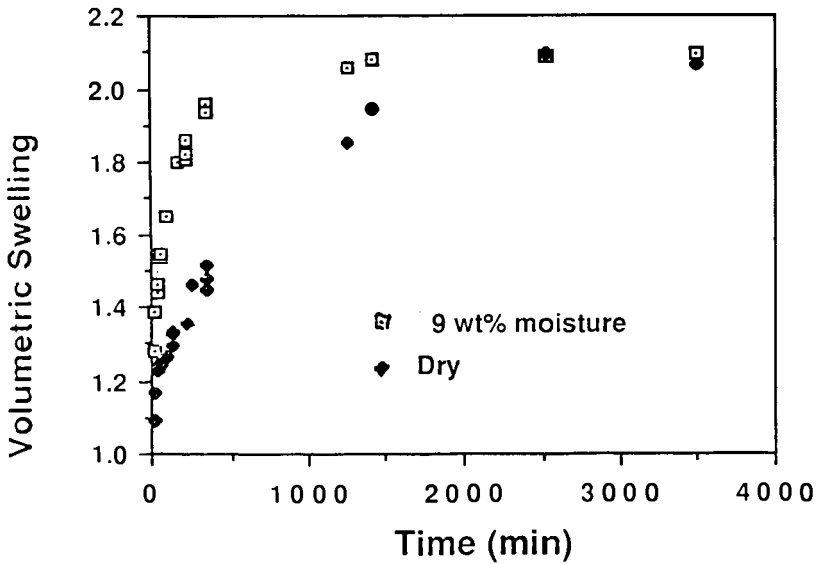
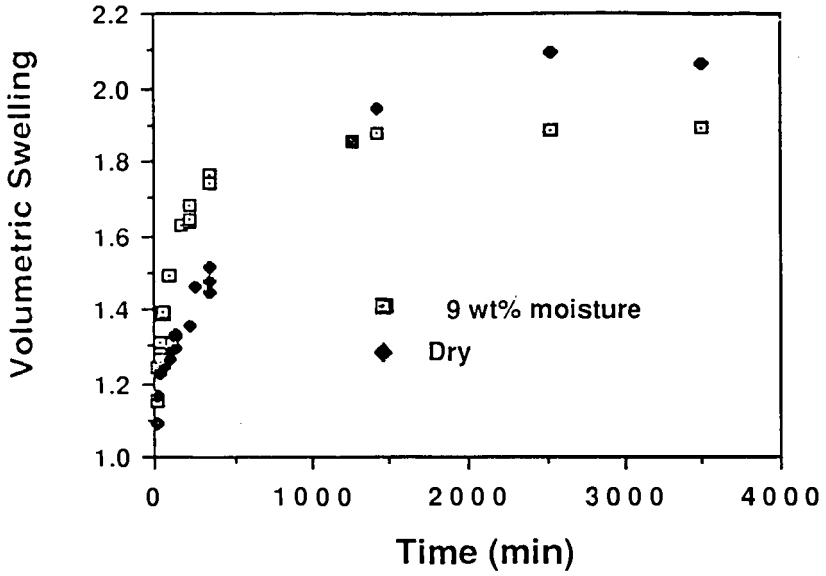


Figure 1. Volumetric swelling ratios ( $Q$ ) in pyridine, at 25°C, of Texas lignite of 212 - 300  $\mu\text{m}$  particle size. Top panel--raw data; lower panel - raw data for moist lignite corrected for water swelling (see text).

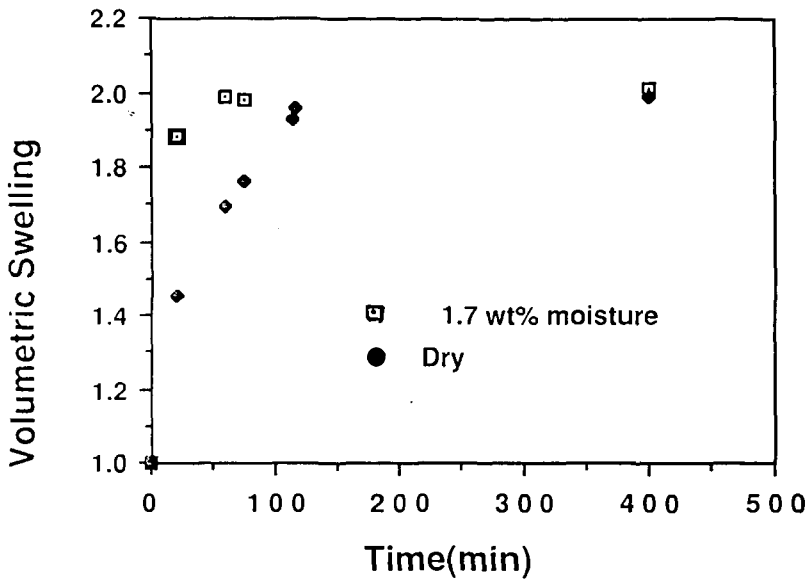


Figure 2. Volumetric swelling ratios (Q) in pyridine, at 25°C, of Powhatan No. 5 high volatile bituminous coal.

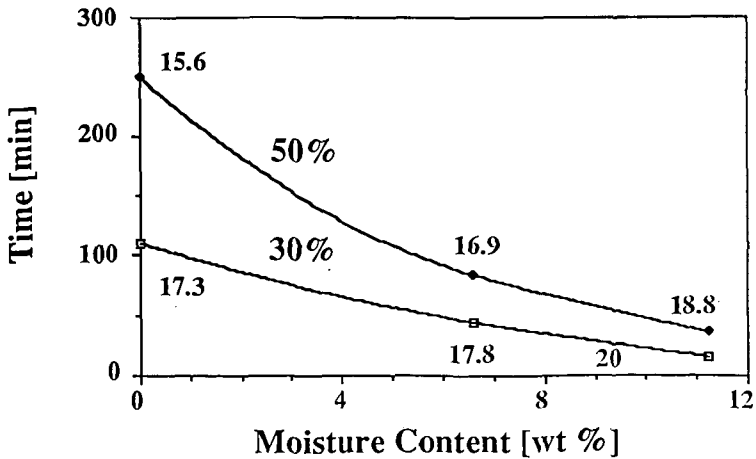


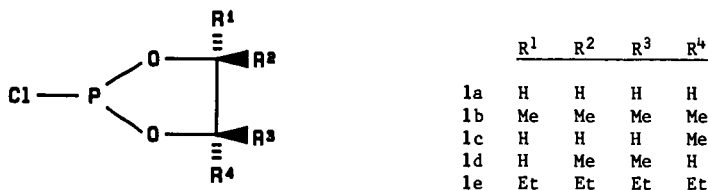
Figure 3. Swelling behavior of Beulah lignite in pyridine at 35°C. The ordinate shows the time required to achieve 30% or 50% of final extent of swelling, as a function of the initial moisture content of the samples. The values next to data points are activation energies for swelling (Kcal/mol).

IDENTIFICATION OF LABILE-HYDROGEN FUNCTIONALITIES  
IN COAL-DERIVED LIQUIDS BY  $^{31}\text{P}$  NMR SPECTROSCOPY

C. Lensink and J. G. Verkade  
Fossil Energy Program, Ames Laboratory  
and  
Department of Chemistry, Iowa State University  
Ames, IA 50011

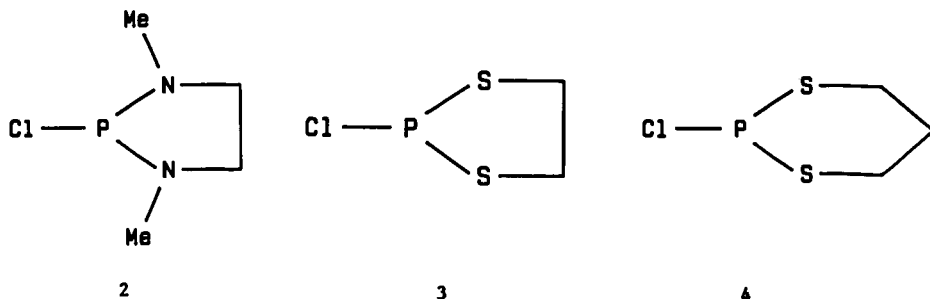
INTRODUCTION

In recent publications from our laboratories<sup>1-3</sup>, the application of  $^{31}\text{P}$  Fourier transform nmr spectroscopy to the analysis of -OH, -NH and -SH functionalities in coal extracts and pyrolysis condensates has been described. We initiated these studies with a series of reagents 1a-e which contain two oxygen atoms in the five-membered phospholane ring system, and varying degrees of ring substitution.



These reagents react under mild conditions with the above labile-hydrogen functionalities,  $\text{R}_\text{X}\text{EH}$  to give  $\text{R}_\text{X}\text{EP}$  linkages in which the phospholane ring remains intact. The HCl liberated is neutralized by triethyl amine in the reaction mixture. In the series 1a-e, reagents 1a and 1b emerged as optimum in terms of minimum overlap of the ranges for each functional group and for maximum resolution within each range of the chemical shifts due to the various R groups attached to the functional group heteroatom E (Figure 1).

To determine the role of the heteroatoms within the ring system of the reagent and the size of the ring system, we are extending our investigations to include reagents such as 2 - 4. Here we describe our preliminary results with a series of model compounds derivatized with these reagents, and also with a coal low-temperature pyrolysis condensate which was allowed to react with 3.



## EXPERIMENTAL

Reagents 2,<sup>4</sup> 3<sup>5</sup> and 4<sup>6</sup> were prepared according to published syntheses. Chemical shift data for derivatized model compounds were obtained by using a procedure described previously.<sup>2,3</sup> For 2 and 3, chemical shift data for the individual model compounds were recorded. For reagent 4 only chemical shift ranges for model compounds were recorded by derivatizing mixtures of phenols, alcohols, acids or amines. The compositions of the mixtures are given in Table I.

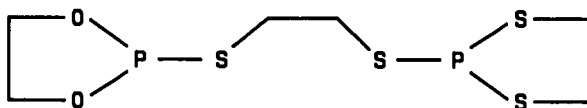
A low-temperature pyrolysis condensate of a Illinois No. 6 coal sample was obtained as described previously.<sup>2,3</sup>

## RESULTS AND DISCUSSION

The chemical shift data for selected model compounds derivatized with 2 - 4 are given in Table II. The regions associated with the <sup>31</sup>P nmr resonances for the model phenols, aliphatic alcohols, carboxylic acids, amines and thiols derivatized with 2 - 4 are shown in Figure 1.

Derivatization of phenols with 2 - 4 gives the corresponding phospholanes (2, 3) or phosphoranes (4) instantaneously. The observed chemical shift range of 15.2 ppm for phenols derivatized with 3 constitutes a significant improvement over the chemical shift range of approximately 6 ppm reported earlier for dioxaphospholanes 1a - 3.<sup>3</sup> Alcohols derivatized with 3 display chemical shifts in the region 143.4 - 151.8 ppm with most of the signals appearing in the 143.4 - 147.2 ppm range. This range is well separated from the chemical shift range observed for derivatized phenols.

An interesting observation can be made from inspection of the data of derivatized pinacol. Derivatization with 3 gives signals at 108.77 and 214.75 ppm. These signals are outside the range of the other derivatized alcohols. The signal at 108.77 ppm is in the range of thiols derivatized with 3 and the peak at 214.75 ppm is in the range of thiols derivatized with 1a - e<sup>3</sup>. These results are consistent with the suggestion that with 1,2-diols, transesterification occurs to give 5.



Carboxylic acids react rapidly with reagents 2 - 4. The chemical shift range for carboxylic acids derivatized with 4 could be obtained for a mixture of acids but within a few minutes signals in the range 61.7 - 1.7 ppm started to appear. It is presently not clear what further reactions may be leading to these signals. The chemical shift range observed for carboxylic acids derivatized with 3 overlaps with the region observed for derivatized phenols (Figure 1).

Amines derivatized with dioxaphospholanes of type 1 (e.g., 1a and 1b in Figure 1) generally give signals in the  $^{31}\text{P}$  nmr spectrum in regions that overlap with signals observed for derivatized -OH functionalities. Amines derivatized with 3, however, give signals well outside the region for -OH functional groups.

Thiols derivatized with 3 display chemical shifts upfield from derivatized -OH functional groups and downfield from derivatized amines. There also appears to be a separation between aromatic and aliphatic thiols similar to the separation between alcohols and phenols.

Preliminary results with coal-derived liquids derivatized with 3 appear promising. Thus, with an Illinois No. 6 low-temperature pyrolysis condensate (Figure 2) peaks in the 152 - 163 ppm region appear well resolved for identification of specific phenols.

#### CONCLUSIONS

Of the three new reagents, reagent 2 does not give an improvement over reagents of type 1. Reagent 2 gives broader  $^{31}\text{P}$  peaks, probably owing to the presence of quadrupolar nitrogen nuclei near the nmr-active phosphorus nucleus.

The resolution obtained with reagent 3 is substantially better than any of the reagents investigated so far, paving the way for identification of functional groups and their organic substituents in coal-derived liquids.

Increasing the ring size of the derivatizing reagent from 3 to 4 does not improve the chemical shift ranges observed nor does it lead to less overlap of the functional group chemical shift ranges.

#### ACKNOWLEDGEMENTS

Ames Laboratory is operated for the U. S. Department of Energy by Iowa State University under Contract No. W-7405-ENG-82. This work was supported in part by the Assistant Secretary for Fossil Energy through the Pittsburgh Energy Technology Center.

#### REFERENCES

1. Schiff, D. E., Verkade, J. G., Metzler, R. M., Squires, T. G., and Venier, C. G., Applied Spectrosc., **40**, 348 (1986).
2. Wroblewski, A. E., Markuszewski, R., and Verkade, J. G., Prep. Pap. Am. Chem. Soc. Div. Fuel Chem., **32**, 202 (1987).
3. Wroblewski, A. E., Lensink, C., Markuszewski, R., and Verkade, J. G., Energy and Fuels, submitted for publication.
4. Ramirez, R., Patwardhan, A. V., Kugler, H. J., and Smith, C. P., J. Am. Chem. Soc., **89**, 6276 (1967).
5. Denney, D. B., Denney, D. Z., and Liu, L. T., Phosphorus and Sulfur, **22**, 71 (1985).
6. Nifantiev, E. E., Sorokina, S. F., Borisenko, A. A., Zavalishina, A. I., and Voiobjeva, L. A., Tetrahedron, **37**, 3183 (1981).

Table I. Model Compound Mixtures Used With Reagent 4.

Functional Group Class	Model Compounds in the Mixture
Phenols	<u>m</u> -cresol, <u>p</u> -cresol, 2,3-xyleneol, 2,4-xyleneol, 2,5-xyleneol, 2,3,5-xyleneol, <u>p</u> -methoxyphenol, 2,4,6-xyleneol, 3,4,5-xyleneol, catechol, resorcinol, 2-methylresorcinol, $\alpha$ -naphthol, <u>o</u> -cresol, hydroquinone, <u>m</u> -methoxyphenol, $\beta$ -naphthol, 3-ethylphenol, 2,6-xyleneol, 3,5-xyleneol, phenol.
Alcohols	methanol, benzyl alcohol, benzhydrol, isoamyl alcohol, mandelic acid, 2,3-butanediol, menthol, cyclohexanol, <u>t</u> -butanol, <u>t</u> -amyl alcohol, pinacol.
Acids	benzoic acid, <u>p</u> -toluic acid, 2,4,6-trimethoxybenzoic acid, mandelic acid, terephthalic acid, $\alpha$ -methylcinnamic acid, succinic acid.
Amines	aniline, <u>o</u> -toluidine, proline, carbazole, 2,6-methylaniline, diisopropylamine, N-ethylaniline, pyrazole.

Table II.  $^{31}\text{P}$  Chemical Shifts of Phenols, Alcohols, Acids, Amines and Thiols Derivatized with 2 and 3.

Compounds	Reagents	
<u>Phenols</u>	2	3
2-methoxy-6-methyl phenol	138.4, 136.5	165.24
2,3,6-dimethyl phenol	132.4	160.72
2,6-dimethyl phenol		160.98
guaiacol	135.0	160.45
phenol	131.2	152.51
$\beta$ -naphthol	132.5	154.32
8-quinolol	135.9	167.38
<u>o</u> -cresol		154.78
<u>p</u> -cresol		152.11
<u>m</u> -cresol		152.87
3,5-dimethyl phenol		153.33
2,4-dimethyl phenol		154.20
<u>Alcohols</u>		
methanol	126.4	145.98
benzyl alcohol	127.3	145.11
isoamyl alcohol	126.5	143.41
menthol	133.1	151.78
<u>t</u> -butanol	124.3	145.66
cyclohexanol	129.1	147.17
pinacol	143.4, 114.1, 113.7	108.77, 214.75
<u>Acids</u>		
terephthalic acid	132.7	insoluble product
benzoic acid	131.2	154.55
<u>d</u> -mandelic acid	132.4	152.18
2,4,6-trimethoxybenzoic acid	130.9	159.83
$\alpha$ -methylcinnamic acid	130.3	153.19
<u>Amines</u>		
2,6-dimethylaniline		103.88
<u>o</u> -toluidine		100.61
di-isopropylamine		92.63
N-ethylaniline		99.97
pyrazole		91.43
<u>Thiols</u>		
2-propanethiol		102.16
thiophenol		113.43
<u>o</u> -thiocresol		112.31
3,4-dimethylthiophenol		112.94

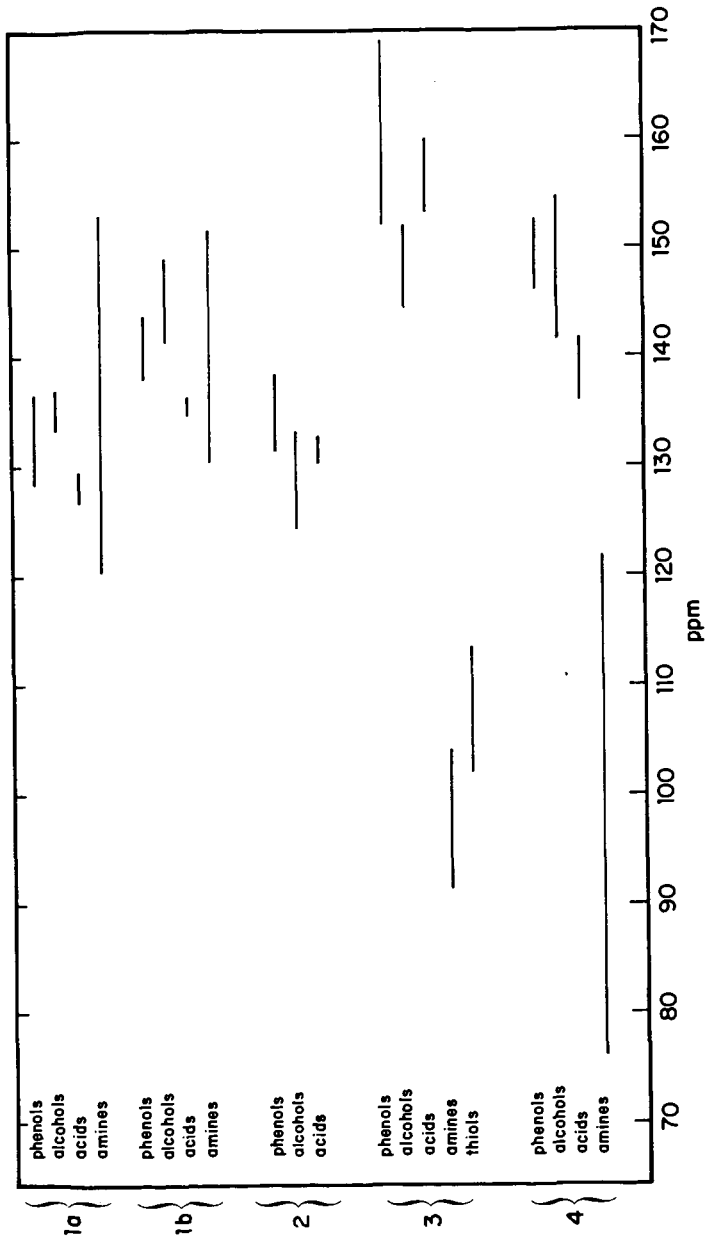


Figure 1. <sup>31</sup>P chemical shift ranges for model compound phenols, alcohols, acids, amines and thiols derivatized with reagents 1a, b and 2 - 4.

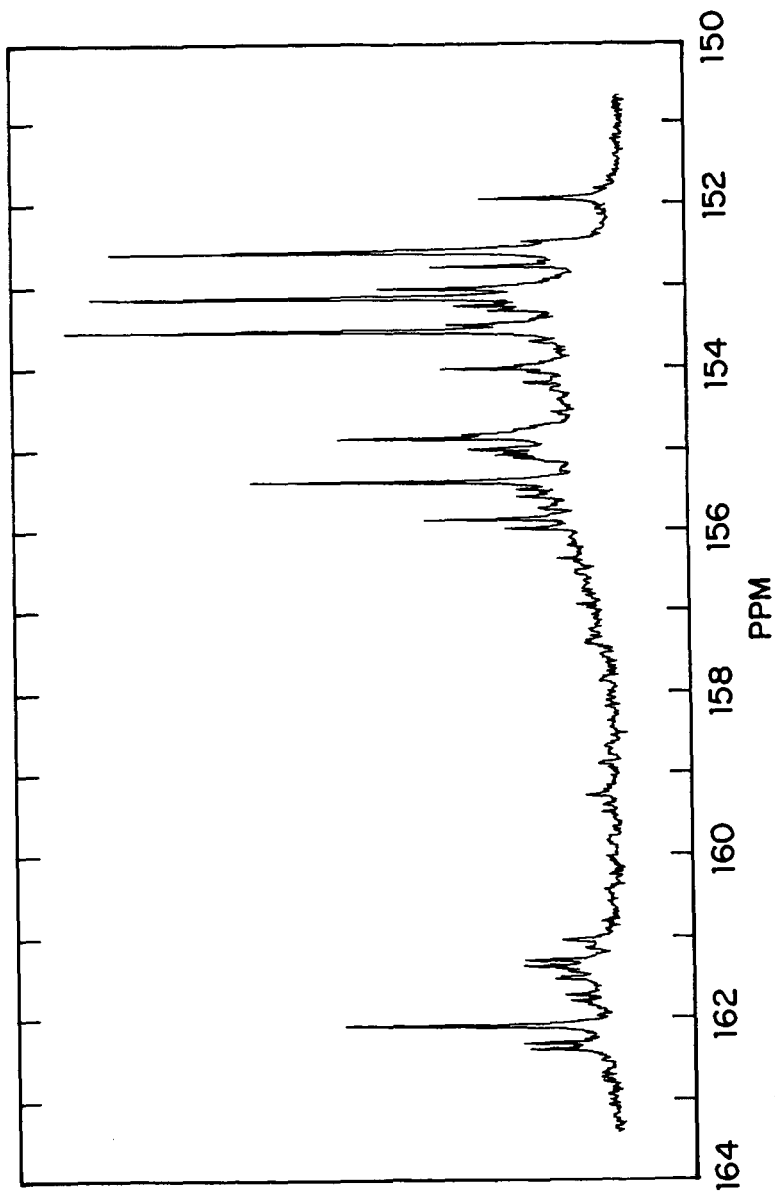


Figure 2.  $^{31}\text{P}$  nmr spectrum of the phenol region of an Illinois No. 6 low-temperature pyrolysis condensate.

## HYDROPROCESSING OF DESALTED DIRECTLY LIQUEFIED BIOMASS

B. Gevert, P. Andersson, \*S. Järås, and S. Sandqvist.  
Department of Engineering Chemistry 1, Chalmers University of Technology,  
S-412 96 GOTHENBURG, Sweden

• EKA Nobel AB, S-445 01 SURTE, Sweden

### ABSTRACT

Desalted directly liquefied biomass from the PERC process was consecutively extracted with iso-octane and xylene. The hydroprocessing was made in a downflow reactor at a constant hydrogen flow and pressure of 85 normal l/h and 10.0 MPa, respectively. The catalyst used was a sulphided cobalt + molybdenum catalyst on gamma alumina. At a liquid flow of 180 ml/h, an hourly liquid space velocity of 1.20 and a temperature of 350°C, the oxygen content of the desalted oil was reduced from 15.3 to 2.3 percent by weight. The effective H/C molar ratio was increased from 1.05 in the starting material to 1.35 and the amount of heavy material with normal atmospheric boiling points above 540°C was reduced from 45.3 to 15.1 percent by weight. Hydroprocessing at 420°C reduced this heavy material further to 4.5 percent by weight. The deoxygenation was only to a small degree dependent on whether the feed oil was desalted or extracted with iso-octane or xylene.

### INTRODUCTION

Hydroprocessing is the most important method to reduce the amount of heteroatoms. Oil produced from biomass contains high amounts of oxygen. Downflow trickle bed reactors are the major type used in hydroprocessing of gas oil and heavier types of petroleum fractions. By using similar systems when upgrading oil produced from biomass, known techniques can be used, thereby achieving lower costs. Furthermore, existing refineries can be used without major rebuilding. Elliott and Baker (1-3) have carried out several experiments in an upflow hydroprocessing reactor. When using a downflow reactor they got severe coking and plugging of the flow. They also claim that at low hold up times, which they used, upflow reactors are better than downflow (1).

Petroleum contains small amounts of inorganic salts, mainly sodium chloride. The inorganic salts will be deposited on heat exchange surfaces and on catalysts in distillation towers. By desalting, the inorganic salts are washed out of the oil. The oil used in this study contains approximately 1% of sodium which is considerably more than what is found in petroleum (4).

Earlier work in our laboratory (5) was based upon the assumption that the crudest part has to be separated out before sensitive hydroprocessing catalysts can be used. Since the oil is more thermally instable than petroleum, extraction has been the method employed. By selecting certain solvents it is possible to receive a predicted yield. However, when separating out the residual part of the oil, large losses occur and the overall yield will be low (4). Therefore, it is of interest to establish a minimum level of amount of residue at which extraction should be performed, without negative effects in the hydroprocessing step.

The purpose of this study was to find a level for suitable yields in the extraction step and still have good conversions without severe deactivation in the hydroprocessing step. Since desalting was included the oil before extraction can also be hydroprocessed. Another important objective was to employ a downflow hydroprocessing reactor. In this paper some preliminary results are presented.

## EXPERIMENTAL

### Feed oils

The feed oil used was produced from Douglas Fir by the PERC Process in test run 13, in the Albany Liquefaction Plant (6). The oil was mixed with 10 percent by weight of iso-octane, desalted with water at 95°C at a ratio of 1 part oil to 2 parts of water (by volume). It was settled overnight and the desalting was repeated once (referred to as oil D). The sodium content of the feed oil was in this way reduced from 0.92 percent by weight to 0.12 percent. Oil D was consecutively extracted with iso-octane and xylene. The solvents were stripped from the extract in a thin film distillation unit (KDL4 Leybold Heraeus). The two oils will be referred to as oil O and oil X respectively. The residue from the extraction was not treated further. Carbon disulphide was added to the feed oils before hydroprocessing to approximately 100 ppm by weight. The reason for this was to maintain a constant activity and selectivity of the sulphided catalyst (2, 7).

### Catalyst

The catalyst used was CoMo on gamma alumina containing 4.2 % CoO and 15.0 % MoO<sub>3</sub> (Akzo Ketjen 742). Prior to use, the catalyst was sulphided with a mixture of 13% hydrogen sulphide in hydrogen at 315°C, 0.3 MPa total pressure and 7 hours of reaction time. In each run 150 ml of catalyst was diluted with 50 ml of carborundum.

### Reactor system

The reactor system was a continuous downflow tricle bed designed by Cities Service and modified for heavy feed stocks. The oil was preheated in the feed tank and further heated in the fluidized sandbath before entering the reactor. The liquid product was stripped after reaction (Figure 1).

### Analysis

Carbon and hydrogen were determined with a LECO CHN-600 instrument. Oxygen and sulphur were determined with a LECO RO-116 and a LECO SC-132 respectively. Material balance of the liquid products were calculated based on determinations on GC (HP 5880) and GPC according to procedure in reference 4. Coke on catalyst was measured after sohxlet extraction with xylene for 24 hrs. and vacuum drying for 24 hrs. at 110°C. A blank value of 2.04% was reduced from the measurement.

## RESULTS AND DISCUSSION

### Results of feed stock characterization

Oil O has a higher H/C ratio and a lower oxygen content than the other oils, see Table 1. The fraction of oil O boiling above 540°C is also considerably lower. Thus oil O has good characteristics for being upgraded. Oil D has a higher oxygen content and a poorer H/C ratio than the other two oils. Finally, oil X has the same low H/C ratio as oil D but a considerably lower oxygen content, 9.5 versus 15.5 for oil D.

### Results of hydroprocessing

Hydroprocessing of the three oils under similar conditions improved the H/C ratio of all oils but, surprisingly, most in oil D (Tables 1 and 2). Oil O seems to be less active than the other two oils in the HDO reactions since the oxygen content is reduced from 8.2 to 4.8 percent while the reduction of oxygen is higher in the other two oils. The experiments also show that oil O is not cracked to the same degree as the other two oils (Table 3). In biomass the cellulose is built by connecting glucose molecules through C - O - C linkages. Furthermore, lignine is connected with C - O - C bindings although less frequently than in cellulose. A material of the liquefied biomass with large molecules is likely to have large amounts of C - O - C bindings remaining. The C - O - C bindings are easier to break than

C - C bindings in hydroprocessing. This might explain the higher reduction of oxygen and molecular sizes of oil D than that of the other two oils. The residue from the extraction of the feed oil was not further tested since the viscosity was too high. By comparing the cracking and deoxygenation of oil O, X and D and the fact that oil O, X and the residue from extraction together forms oil D. The residue must show a higher activity for cracking and deoxygenation than oil O, X and D. However, on the other hand there might be components in oil O and X which are necessary for deoxygenation and cracking of the residue from extraction.

The largest surface area of the catalyst is found in pores with a diameter between 25 - 80 Å. For a complete pore distribution of the catalyst used, see reference 8. Larger molecules will be limited by diffusion and even not able to enter the smallest pores. The conversion of the largest molecules ( $C_{44+}$ ) is a strong indication that thermal reactions or homogenous catalysis is important (Table 3). When hydroprocessing in another system, Gevert and Otterstedt (8) showed high conversions without any catalyst present.

Coke on catalyst was measured after the runs and showed high amounts in all cases (Table 4). The high amounts of coke on the catalyst from the experiment with oil O cannot be explained with the limited amounts of experiments in this preliminary study.

In a special run (No. 1) with oil D, a higher temperature, 420°C, was used instead of 350°C (Table 1 and 2). The higher temperature gave considerably more coke on catalyst, 24%, as compared to 11% for the lower temperature (run No. 2). The conversion of heavier material ( $C_{44+}$ ) was also much higher which has also been found earlier.

#### CONCLUSIONS

Downflow hydroprocessing of desalted oil from biomass has been successfully done. The preliminary experiments indicate that the residue after extraction with iso-octane and xylene has a higher activity in hydro-deoxygenation and cracking than the extracted oils. Extraction before hydroprocessing is not necessary.

#### ACKNOWLEDGEMENT

The authors gratefully acknowledge the Swedish National Board of Energy who sponsored this project.

#### LITERATURE CITED

1. Elliott, D.K., Baker, E.G. Biotechnology and bioengineering Symposium. 1984, No. 14, 159-174.
2. Elliott, D.C., Baker, E.G. in Proceedings of the 17th Biomass Thermochemical Conversion Contractors Meeting, 1985, CONF-8510167, NTIS 1985.
3. Baker, G.B., Elliott, D.C. Preprint paper - American Chemical Society, Div. Fuel Chemistry. 1987, 32, No. 2, 257-263.
4. Gevert, S.B. Refining of directly liquefied biomass to transportation fuels, IGT Conference on Energy from Biomass and Wastes X, Orlando, March 16-20, 1987.
5. Gevert, S.B., Otterstedt, J-E. Upgrading of liquefied biomass to transportation fuels by extraction. IGT Conference on Energy from Biomass and Wastes X, Washington D.C., April 7-10 1986.
6. Thigpen, P.G., Berry, W.L. In reprints IGT Conference on Energy from Biomass and Wastes VI, Lake Buena Vista, Florida, January 25-29 1982. pp. 1057-1095.

7. Gevert, S.B., Otterstedt, J-E., Massoth, F.E. Applied Catalysis, 1987, 31, 119-131.
8. Gevert, S.B., Otterstedt, J-E. Biomass, 13, 1987, 105-115.

**Table 1** Experimental conditions in the different runs

Run No.	1	2	3	4
Oil	D	D	X	O
Temperature (°C)	420	350	350	350
Oil flow (ml/h)	170	180	170	110
LHSV	1.7	1.2	1.13	0.79
Experimental time (h)	6	6	6	6

**Table 2** Elemental composition (in weight percent) of the different oils before and after experiments

Oil/Element	C	H	O	H/C*
D	70.6	8.2	15.5**	1.00
X	81.0	8.2	9.5	1.04
O	80.6	9.4	8.2	1.29
1	76.8	10.2	3.1	1.53
2	85.9	10.4	2.3	1.41
3	86.5	9.8	2.5	1.32
4	84.3	9.8	4.8	1.31

\*The hydrogen to carbon ratio has been calculated under the assumption that the present oxygen consumes the hydrogen.

\*\*Part of this 15.5 % of oxygen is due to organic oxygen in the oil, some remaining salts and also partly due to oxygen in the water.

**Table 3** Boiling point characteristics of the oils in weight percent (values have been normalized)

Oil/Interval	-C <sub>4</sub>	C <sub>4</sub> -C <sub>12</sub>	C <sub>13</sub> -C <sub>20</sub>	C <sub>21</sub> -C <sub>44</sub>	C <sub>44</sub> +
D	0	1.7	25.0	42.1	31.2
X	0	2.9	31.6	44.7	20.8
O	0	5.0	49.3	42.8	2.9
1	0	18.0	43.1	34.6	4.3
2	0.1	20.0	36.5	29.8	13.6
3	0.2	17.9	37.7	29.7	14.5
4	0	13.3	45.9	33.5	7.32

**Table 4** Coke on catalyst in weight percent and hydrogen consumption in vol. hydrogen/vol. oil.

No.	Coke	Hydrogen consumption
1	24.0	-
2	11.0	-
3	11.1	152
4	21.4	81

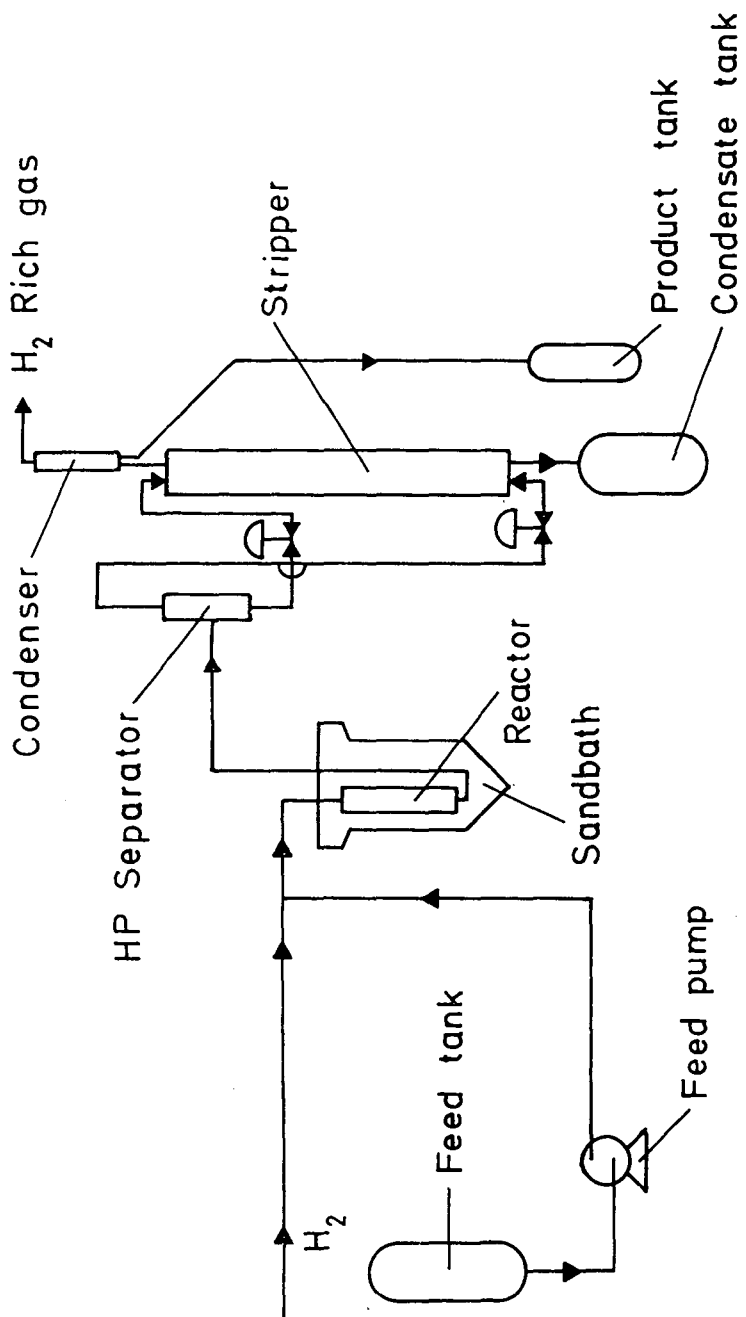


Fig.1 Principle flow diagram of hydroprocessing equipment.

# SIMULATED DISTILLATION AND MOLECULAR WEIGHT DETERMINATION BY SUPERCRITICAL FLUID CHROMATOGRAPHY

S. Coulombe and G. Duquette

CANMET, Energy, Mines and Resources Canada  
555 Booth St.  
Ottawa, Canada K1A 0G1

## INTRODUCTION

Supercritical fluid chromatography (SFC) has recently become a popular technique for the analysis of crude oils. It has been demonstrated for simulated distillation (1) and for hydrocarbon type separation (2-3). The advantages of SFC over gas chromatography (GC) in simulated distillation are the wider boiling range and lower temperature thus preventing cracking of heavy molecules during analysis. Previous work with GC (4) has shown that average molecular weight can be determined for aromatic fractions using a technique similar to simulated distillation. The present study on retention time behaviour of standard compounds shows how the same approach can be applied to SFC. Correlations between retention times and boiling point, molecular weight and melting point have been studied.

## EXPERIMENTAL

A Lee Scientific Model 600 SFC/GC was used. The separations were performed on a 10 m x 100  $\mu$ m i.d. DB-5 column (for naphtha range) and two 10 m x 100  $\mu$ m DB-5 column (for heavier standards) from J&W Scientific, Inc, using carbon dioxide as the mobile phase. The end of the column was connected to a frit restrictor inserted in a 100  $\mu$ m i.d. fused silica sleeve. The restrictor was directly inserted in the FID detector. The following pressure or density ramps were used: for the naphtha range (IBP- 200°C), initial pressure of 80 atm for 5 min, followed by a 1 atm/min ramp to 200 atm; for the middle distillate range (200- 350°C), initial density of 0.1444 g/mL for 7.5 min, followed by a ramp of 0.0092 g/mL/min to 0.5930 g/mL; for the gas oil range (350- 525°C), initial density of 0.3095 g/mL for 5 min, followed by a ramp of 0.006 g/mL/min to 0.7411 g/mL. All runs were isothermal at 100°C. Sample introduction was made via a Rheodyne 7520 valve having a 0.5  $\mu$ L injection volume.

## RESULTS AND DISCUSSION

### 1- Boiling point

As would be expected from literature on simulated distillation by SFC (1), there is a very good correlation between retention time and boiling point. However, in the light naphtha range, the calibration is not linear. Thus, the pressure (or density) program must be adjusted to provide a linear relation or a proper calibration procedure must be used in order to accurately determine the initial boiling point of a sample. It should be noted that the inflexion point is at about the operating temperature. From this result, it appears that a temperature program would be useful for an adequate calibration of the lighter portion of the sample (low initial temperature) and of the heavier portion (high final temperature).

### 2- Molecular weight

A previous study (4) has shown that the molecular weight of aromatic fractions from topped (light fractions removed) crude oils can be evaluated by a technique similar to simulated distillation. In that work, after hydrocarbon type separation by column chromatography the aromatics fraction was separated by GC on a non-polar column. Since the compounds are of the same type, boiling points and molecular weights were both well correlated to retention time. This correlation allowed the determination of the boiling range, the average molecular weight as well as the molecular weight distribution of these fractions. A similar approach with SFC would eventually permit monitoring molecular weight of heavier samples.

As shown in Fig. 2, a poor correlation exists between molecular weight and retention time in the naphtha and middle distillate range, except for straight chain paraffins. However, in the gas oil range, the correlation for non-paraffinic standard compounds is improved. As molecular weight increases, it seems that the influence of the functional group becomes less important compared with molecular weight. This could be due to increased steric hindrance or more electron delocalization over the structure of the molecule which reduces the polarity. Thus, it appears that the molecular weight determination would only be effective for heavy fractions.

### 3- Melting point

Solubility of solids in liquids is determined by intermolecular forces as well as enthalpy of fusion and melting point of the solute (5). Since a supercritical fluid has densities approaching those of a liquid and since the retention time is related to solubility, we investigated how the melting of the solute would be related to the retention time. As shown in Fig. 3, there is no correlation except for the n-paraffins which was expected since their melting point increases regularly with molecular weight.

Melting point was expected to have an influence when the operating temperature was lower than the melting point. All the results shown in Fig. 3 were obtained at 100°C. Although there is some trend in Fig. 3c, there is too much variation to significantly relate melting point and retention time, and the correlation is very poor even within the same family of compounds.

#### 4- Response factors

All simulated distillation techniques assume that the various components of a crude oil sample have nearly identical response factors. Figure 4 shows that response factors can be significantly different. However, within the same class of compounds, it seems that the response factors do not vary to the same extent. Therefore, boiling range determination could lead to erroneous results if the relative quantity of different compound types varies from sample to sample. On the other hand, for hydrocarbon type separation by SFC, results can be reliable if proper response factors are assigned to each compound class. Since the difference between the response factors of saturates and aromatics is small, samples with low heteroatomic content could lead to satisfactory results.

#### CONCLUSIONS

The study of retention behaviour showed that, for given SFC conditions, retention time is mainly dependent on the boiling point of the solute. Some correlation was found with the molecular weight and no significant link was found with the melting point. Response factors were found to vary between compound classes but to be quite consistent within the same class.

#### REFERENCES

1. Schwartz, H.E., Brownlee, R.G., Boduszynski, M.W., and Su, F., Anal. Chem., 59, 1393-1401, 1987.
2. Norris, T.A. and Rawdon, M.G., Anal. Chem., 56, 1767-1769, 1984.
3. Campbell, R.M., Djordjevic, N.M., Markides, K.E. and Lee, M.L., Anal. Chem., 60, 356-362, 1988.
4. Coulombe, S. and Sawatzky, H., Fuel, 65, 552-557, 1986.
5. Reid, R.C., Prausnitz, J.M. and Sherwood, T.K., The Properties of Gases and Liquids, 3rd ed., McGraw-Hill, New York, pp.380-384.

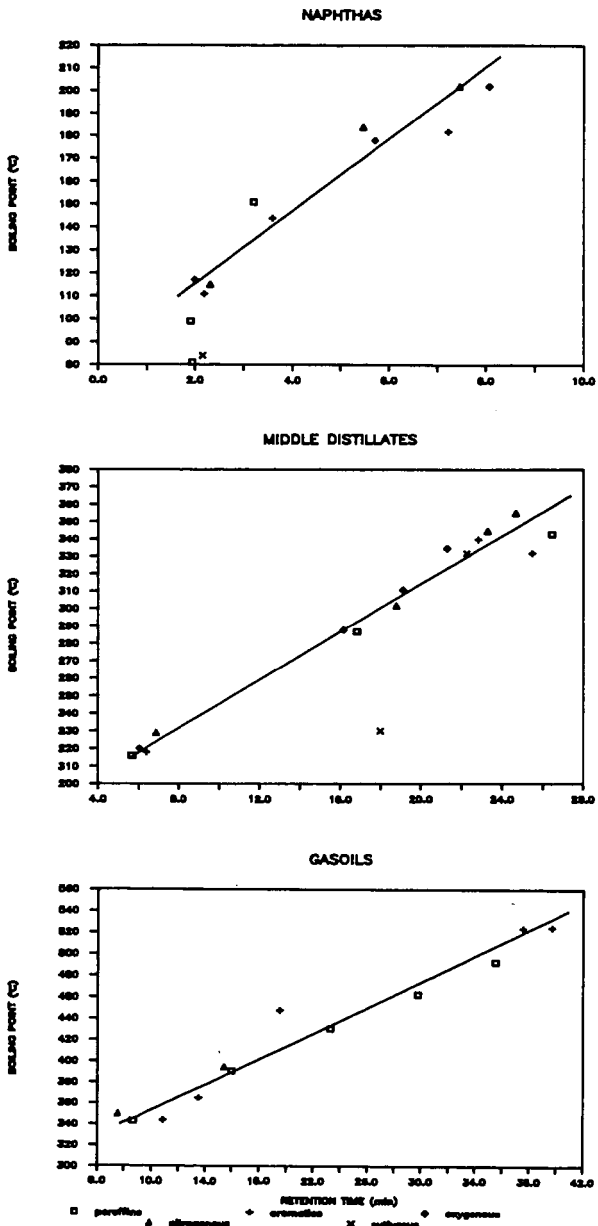


Figure 1 - Correlation between boiling point and retention time

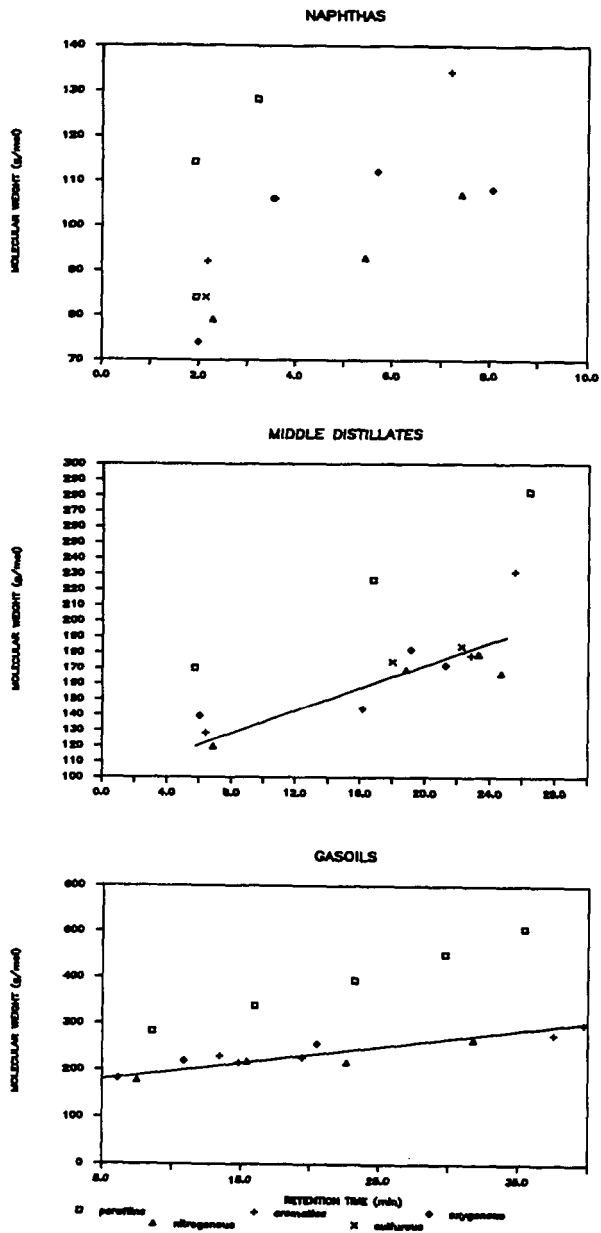


Figure 2 - Correlation between molecular weight and retention time

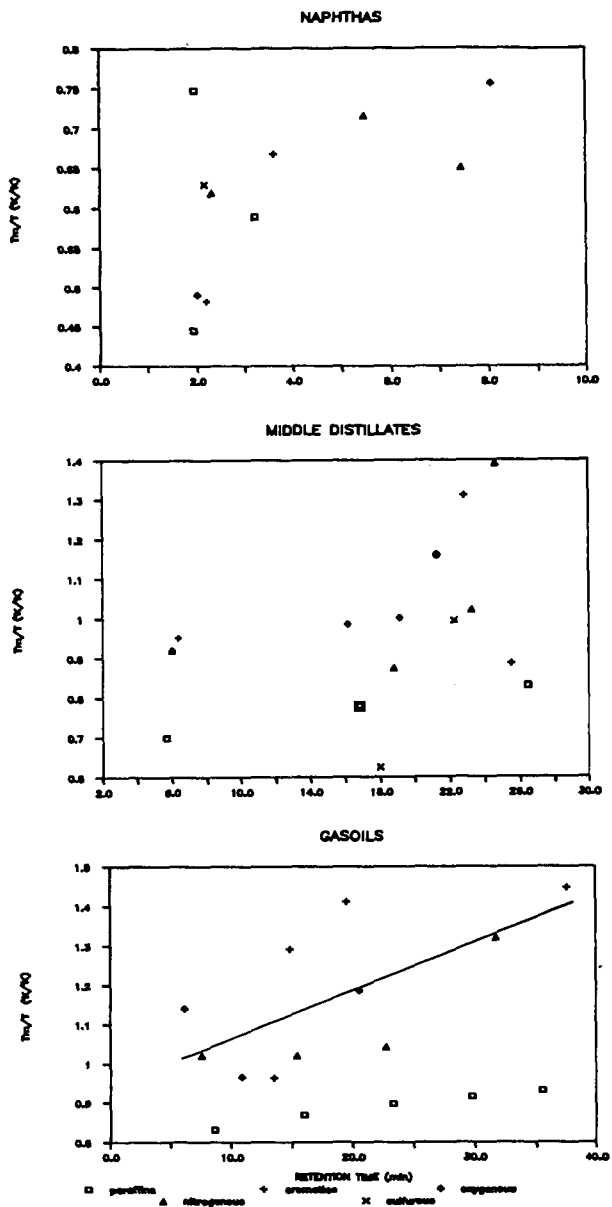


Figure 3 - Correlation between melting point and retention time ( $T_m$ : melting point;  $T$ : operating temperature)

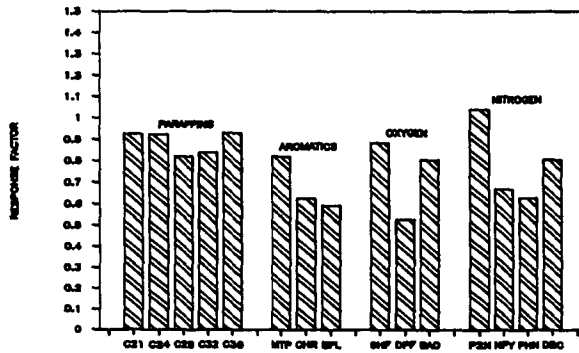
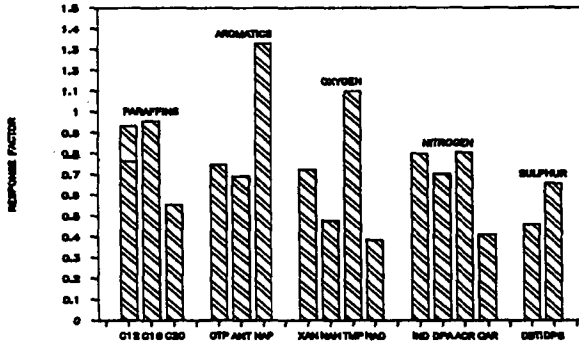
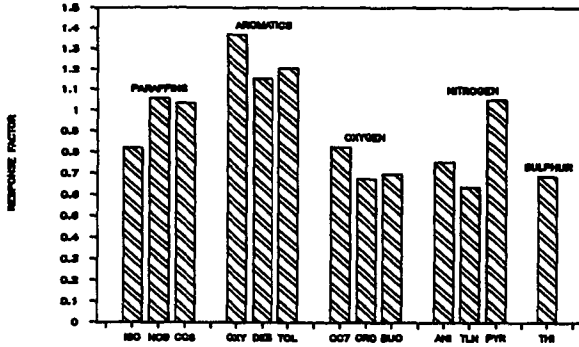


Figure 4 - Response factors (SFC with FID)

ARTIFICIAL SIMULATION OF HYDROCARBON  
GENERATION IN COAL USING HYDROUS PYROLYSIS TECHNIQUES

S. C. Teerman and R. J. Hwang,  
Chevron Oil Field Research  
P. O. Box 446  
La Habra, California 90633-0446

INTRODUCTION

Coal, which is usually land plant in origin, occurs in many oil-producing basins. Microscopically, coal consists of various macerals (liptinite, vitrinite, and inertinite). The generative potential of coal reflects the hydrocarbon potential of the composing macerals (Kelly et al., 1985). Although most coals consist of predominantly vitrinite, some contain significant amounts (>20% of total maceral content) of oil-prone liptinite macerals. Work by Brooks and Smith, 1967; Connan, 1974; Durand and Paratte, 1982; Thompson et al., 1985; and MacGregor and McKenzie, 1986 suggests that certain coals can be considered as source rocks for liquid hydrocarbons. Their conclusions are based on the close association of coal with liquid hydrocarbon occurrences and promising source potential supported by various geochemical analyses. However, the liquid hydrocarbon potential of coal cannot easily be evaluated because of its variable maceral composition, its unique occurrence compared to most source rocks, and difficulty in quantifying liquid hydrocarbon expulsion.

The overall objective of this study is to complete hydrous pyrolysis experiments to evaluate the liquid hydrocarbon potential of coal. Specific aspects of this study include: (1) a quantitative assessment of the generative potential of coal, and (2) an evaluation of the composition of liquid hydrocarbons generated from coal at various temperatures.

EXPERIMENTAL

Original (Unheated) Samples

Hydrous pyrolysis experiments were completed using Tertiary lignites from North Dakota and the Far East. Both lignites are thermally immature ( $R_o < 0.35\%$ ) with respect to hydrocarbon generation. The Far East lignite is liptinite-rich (32% of total maceral content), which is supported by elemental analysis ( $H/C=1.0$ ) and Rock-Eval pyrolysis (Hydrogen Index=483 mg HC/g O.C.). Resinite is the most abundant liptinite maceral (13.7%) in the Far East sample. The North Dakota lignite is vitrinite-rich (95% of total maceral content) and

liptinite-poor (3%). Geochemical and microscopic data for the two unheated lignites are listed in Table 1.

### Methods and Procedures

Hydrous pyrolysis was used to evaluate product yields, compositions, and the temperature of liquid hydrocarbon generation from the two lignites. This technique has been suggested as a method that best simulates source rock burial and the natural generation and expulsion of petroleum (Lewan et al., 1979; Lewan, 1983; and Winters et al., 1981). These studies suggest that oil-pyrolysate formed under hydrous pyrolysis conditions closely resembles naturally generated products because of the presence of water at high temperatures and pressures in a closed system. However, other pyrolysis methods (closed system anhydrous) can also simulate petroleum generation. Monthioux et al., 1985 suggests that closed-system pyrolysis of coals more closely simulates natural maturation than open-system pyrolysis techniques.

Hydrous pyrolysis procedures used were similar to those described by Lewan et al., 1979. Both lignites were crushed to 0.5 to 1.0mm chips, sieved to remove fines, and thoroughly homogenized. Individual samples were heated to temperatures ranging between 250 and 360°C for 72 hours in 1-liter stainless steel reactors. Both floating and sorbed (solvent rinsed) pyrolysate, as described by Lewan (1983), were included as expelled product. The pyrolyzed lignite residues were geochemically and microscopically characterized to evaluate changes that occur during artificial maturation.

## RESULTS AND DISCUSSION

### Quantity of Generated Oil-Pyrolysate

A maximum of 48 and 158 mg/g O.C. of oil-pyrolysate is generated from the North Dakota and Far East lignites, respectively (Table 2). Peak generation occurs at 340 and 360°C for the North Dakota and the Far East lignite, respectively (Figure 1). Expelled products consist predominantly of sorbed pyrolysate (Table 2). The differences in oil-pyrolysate yield and temperature of peak generation for the two lignites are probably related to the quantity and type of oil-prone liptinite macerals.

Peak generation temperature for the Far East sample is probably influenced by resinite. Lewan (1987) and Hwang and Teerman (1988) document that large amounts of oil-pyrolysate are generated from resinite, with peak generation occurring at, or above 360°C. Based on a hydrous pyrolysis experiment of a representative sample of solvent (methylene chloride)

extracted Far East lignite (to remove soluble resinite), approximately half of the oil-pyrollysate originates from resinite (Table 2).

### Oil-Pyrollysate Composition

Although oil-pyrollysate composition varies with temperature, the pyrollysates generally display a significant amount of n-paraffins and light aromatic and naphthenoaromatic components. Comparison of the Far East and North Dakota oil-pyrollysates at various temperatures are shown in Figures 2 and 3. These oil-pyrollysates are similar to some naturally occurring non-marine oils.

Below 290°C, the Far East oil-pyrollysates are dominated by sesquiterpenoid components, such as cadalene and other alkyl naphthalenes (Figure 2). These (sorbed) oil-pyrollysates consist of soluble resinite rather than a "thermally generated" product. Solvent rinsing the unheated Far East lignite results in a similar quantity of sorbed product. Below 290°C, the North Dakota oil-pyrollysate is dominated by light aromatic and naphthenoaromatic components and contains small amounts of n-paraffins (Figure 3).

Above 290°C, both oil-pyrollysates contain significant amounts of n-paraffins, ranging from  $C_{10}$  to about  $C_{32}$ . Although the odd/even predominance in both oil-pyrollysates decreases with temperature, it is still evident at 360°C. Precursors of n-paraffins consist of cutinite, sporinite, and other liptinite macerals, which contain plant waxes (Brooks and Smith, 1967 and Nip et al., 1988). Liptodetrinite and submicroscopic inclusions of bacterial, algal, and plant lipids in desmocollinite (a vitrinite maceral) probably contribute to the n-paraffins. Differences in the distribution and relative abundance of n-paraffins in the two oil-pyrollysates (Figures 2 and 3) are probably related to variation in their precursors.

In the  $C_6$ - $C_{15}$  range there is also a significant amount of aromatic and naphthenoaromatic products. These originate mainly from vitrinite and resinite. The Far East oil-pyrollysates display significant amounts of  $C_2$ - to  $C_5$ -alkyl naphthalenes, which are similar in distribution to a resinite oil-pyrollysate, described by Hwang and Teerman, 1988. This suggests the importance of resinite as a precursor for the Far East naphthenoaromatic components. Generated products from resinite in the Far East lignite are non-paraffinic consisting of cyclic isoprenoids and their aromatic derivatives.

Phenols also occur in significant amounts in both oil-pyrollysates. These compounds are probably derived from

diagenetically altered lignin precursors in vitrinite and inertinite (Chaffee et al., 1984). However, some liptinite macerals (sporinite) may generate phenolic compounds (Meuzelaar et al., 1984). Resinite does not generate phenolic compounds (Hwang and Teerman, 1988). The presence of phenol and alkylphenols in these oil-pyrollysates indicates a contribution from the lignin precursors. However, the contribution to the total oil-pyrollysate is small relative to that of the wax and resin components. The North Dakota lignite yields relatively larger amounts of phenols compared to the Far East sample. This observation is consistent with the vitrinite-rich maceral composition of the North Dakota lignite.

#### Characterization of Heated Lignites

Atomic H/C and O/C ratios generally decrease with temperature (Table 3). Thermally altered Far East samples plot at the top of the van Krevelen Type III pathway; North Dakota samples plot between the Type III and IV pathways (Figure 4).

Maceral analysis of the Far East samples suggests that hydrocarbon generation from individual liptinite macerals occur at different temperatures. Except for resinite, almost all liptinite macerals have disappeared by 330°C. At 350°C only small amounts of resinite remain. Secondary products consisting of exsudatinite and bitumen smear films still occur at 360°C.

Vitrinite reflectance values increase exponentially with a linear increase in temperature (Figure 5). Differences in the reflectance profiles of the two lignites are probably related to the vitrinite precursor.

#### Generative Potential of Coal

Based on these hydrous pyrolysis results, coals that contain small to moderate amounts of liptinite (<20% total maceral content) cannot generate significant amounts of liquid hydrocarbons. The contribution of desmocollinite to the liquid hydrocarbon potential of coal in a natural system is uncertain.

The Hydrogen Index of the unheated Far East lignite (483 mg HC/g O.C.) is similar to some Type II kerogens. However, the quantity of generated product is much less than that from hydrous pyrolysis experiments of Type II kerogens, reported by Lewan (1985) and K. E. Peters (personal communication). The large discrepancy in the quantity of generated pyrollysate between Rock-Eval and hydrous pyrolysis (483 versus 158 mg/g O.C.) can be attributed to the different

methods of measuring pyrolysate quantity and pyrolysis techniques (open- versus closed-system). Caution must be used in directly relating Rock-Eval Hydrogen Index to the source potential of coal.

Although the composition of the North Dakota oil-pyrolysate is similar to some naturally occurring waxy oils, the quantity of generated product is insignificant compared to most source rocks. Both the quantity and composition of an artificially generated product must be considered when evaluating the source potential of coal.

## REFERENCES

- Brooks, J. K. and Smith, J. W. (1967). The diagenesis of plant lipids during the formation of coal, petroleum and natural gas. I. Changes in the n-paraffin hydrocarbons. *Geochimica. Cosmochimica Acta*, v. 31, p. 2389-97.
- Chaffee A. L., Johns R. B., Baerken M. J., de Leeuw J. W., Schenck, P. A. and Boon J. J. (1984). Chemical effects in gelification processes and lithotype formation in Victorian brown coal. In *advances in organic geochemistry, 1983* (eds. P. A. Schenck, J. W. de Leeuw and G. W. M. Lijmbach). *Org. Geochem.* 6, p. 409-416.
- Connan, J. (1974). Natural diagenesis and artificial diagenesis of organic matter of predominantly plant constituents. Tissot, B. and Bienner, F., Eds. *Advances in organic geochemistry, proceeding of the 6th International meeting on organic geochemistry, 1973*, p. 73-95.
- Durand, B. and Paratte, M. (1982). Oil potential of coals: A geochemical approach: *Symp. Petroleum Geochemistry and Exploration of Europe*, J. Brooks, editor, Blackwell Scientific Publications, Oxford, England, p. 285-292.
- Hwang, R. J. and Teerman, S. C. (1988). Hydrocarbon characterization of resinite. *Journal of Energy and Fuels* 2, p. 170-175.
- Kelly, P. A., Bissada, K. K., Burda, B. H., Elrod, L. H., and Pheifer, R. H. (1985). Petroleum generation potential of coals and organic rich deposits: significance in Tertiary coal rich basins: *Indonesian Petroleum Association Proceedings, 14th Annual Convention*, v. 1, p. 1-21.
- Lewan, M. D., Winters, J. C. and McDonald, J. H. (1979). Generation of oil-like pyrolyzates from organic-rich shales. *Science*, v. 203, p. 897-899.
- Lewan, M. D. (1983). Effects of thermal maturation on stable organic carbon isotopes as determined by hydrous pyrolysis of Woodford shale. *Geochim. Cosmochim. Acta*, v. 47, p. 1471-1479.
- Lewan, M. D. (1985). Evaluation of petroleum generation by hydrous pyrolysis experiments. *Phil. Trans. of the Royal Soc.*, v. 315, p. 123-134.
- Lewan, M. D., and Williams, J. A. (1987). Evaluation of petroleum generation from resinites by hydrous pyrolysis: *AAPG Bull.*, v. 71, p. 207-214.

- MacGregor, D. S. and McKenzie, A. G. (1986). Quantification of oil generation and migration in the Malacca Strait region of central Sumatra. Proceedings Indonesian Petroleum Association, 1986, v. 1, p. 305-320.
- Meuzelaar, H. L. C., Harper, A. M., Pugmire, R. J., and Karas, J. (1984). Characterization of coal maceral concentrates by Curie-point pyrolysis mass spectrometry. Coal Geol., v. 4, no. 2, p. 143-172.
- Monthieux, M., Landais, P., and Durand, B. (1985). Comparison between extracts from natural and artificial maturation series of Mahakam Delta coals. Org. Geochem., v. 10, p. 299-311.
- Nip, M., de Leeuw J. W. and Schenck, P. A. (1988). The characterization of eight maceral concentrates by means of Curie Point pyrolysis-gas chromatography and Curie point pyrolysis-gas chromatography-mass spectrometry. Geochim. Cosmochim. Acta 52, p. 637-648.
- Peters, K. E. Personal communication of unpublished results.
- Thompson, S., Morley, R. J., Barnard, P. C. and Cooper, B. S. (1985). Facies recognition of some Tertiary coals applied to prediction of oil source rock occurrence. Marine and Petroleum Geology, v. 2, p. 288-297.
- Winters, J. C., Williams, J. A., and Lewan, M. D. (1981). A laboratory study of petroleum generation by hydrous pyrolysis. In: M. Bjoroy et al. (eds.), Adv. in Org. Geochem. (1981), John Wiley & Sons, Chichester, U.K., p 524-533.

TABLE 1

CHARACTERIZATION OF UNHEATED FAR EAST AND NORTH DAKOTA  
LIGNITES FOR HYDROUS PYROLYSIS EXPERIMENTS

<u>Total Organic Carbon/Rock-Eval Pyrolysis</u>									
	<u>Wt. % TOC</u>	<u>Mg HC/g rock</u>	<u>Mg HC/g rock</u>	<u>Mg CO<sub>2</sub>/g rock</u>	<u>Tmax °C</u>	<u>S1 S1+S2</u>	<u>S2/S3</u>	<u>Hydrogen Index Mg HC/g O.C.</u>	<u>Oxygen Index Mg CO<sub>2</sub>/g O.C.</u>
Far East	55.01	21.31	265.80	14.06	390	0.07	18.90	483	25
North Dakota	55.29	6.90	67.80	29.02	389	0.09	2.34	123	52

Elemental Analyses and Microscopy

	<u>Far East</u>	<u>North Dakota</u>
Atomic H/C	1.00	0.94
Atomic O/C	0.23	0.35
% Vitrinite Reflectance	0.33	0.29
Maceral Percent		
% Vitrinite (huminite)	65.9	94.9
% Liptinite	31.8	3.0
Exinite	18.1	2.2
Resinite	13.7	0.8
% Inertinite	2.3	2.1

TABLE 2

QUANTITY OF OIL-PYROLYSATE  
 FAR EAST AND NORTH DAKOTA LIGNITES

Temperature °C	Expelled Pyrolysate		Total Expelled Pyrolysate (mg/g TOC) <sup>2</sup>
	Floating (mg/g TOC) <sup>2</sup>	Sorbed (mg/g TOC) <sup>2</sup>	
<u>Far East</u>			
-250	-	68.0	68.0
-270	-	83.5	83.5
-290	-	95.7	95.7
-310	-	97.0	97.0
-330	-	113.5	113.5
-350	68.8	108.1	152.6
-350 <sup>1</sup>	-	87.9 <sup>1</sup>	87.9 <sup>1</sup>
-360	trace	157.6	157.6
<u>North Dakota</u>			
-260	-	11.4	11.4
-270	-	24.0	24.0
-280	-	17.9	17.9
-290	-	7.1	7.1
-310	-	15.8	15.8
-330	-	6.6	6.6
-340	-	46.7	47.7
-350	-	24.1	24.1
-360	-	31.1	31.1

<sup>1</sup> Solvent-extracted lignite

<sup>2</sup> Based on organic carbon value of 64.65 and 63.11 for  
 Far East and North Dakota lignites from elemental analysis

TABLE 3

ELEMENTAL ANALYSES AND VITRINITE REFLECTANCE  
DATA FOR RESIDUAL (HEATED) FAR EAST AND  
NORTH DAKOTA LIGNITE SAMPLES

<u>Temp. °C</u>	<u>Atomic H/C</u>	<u>Atomic O/C</u>	<u>% Ro</u>
<u>Far East</u>			
Original	1.00	0.23	0.33
250	1.01	0.15	0.57
270	1.05	0.13	-
290	0.97	0.12	0.72
310	0.92	0.10	-
330	0.91	0.07	1.01
350	0.72	0.06	1.34
<u>North Dakota</u>			
Original	0.94	0.35	0.29
260	0.77	0.25	0.60
270	0.78	0.22	0.70
280	0.71	0.20	0.77
290	0.68	0.20	0.80
310	0.66	0.13	1.08
330	0.68	0.10	1.28
340	0.64	0.10	1.40
350	0.61	0.09	1.45
360	0.60	0.08	1.58

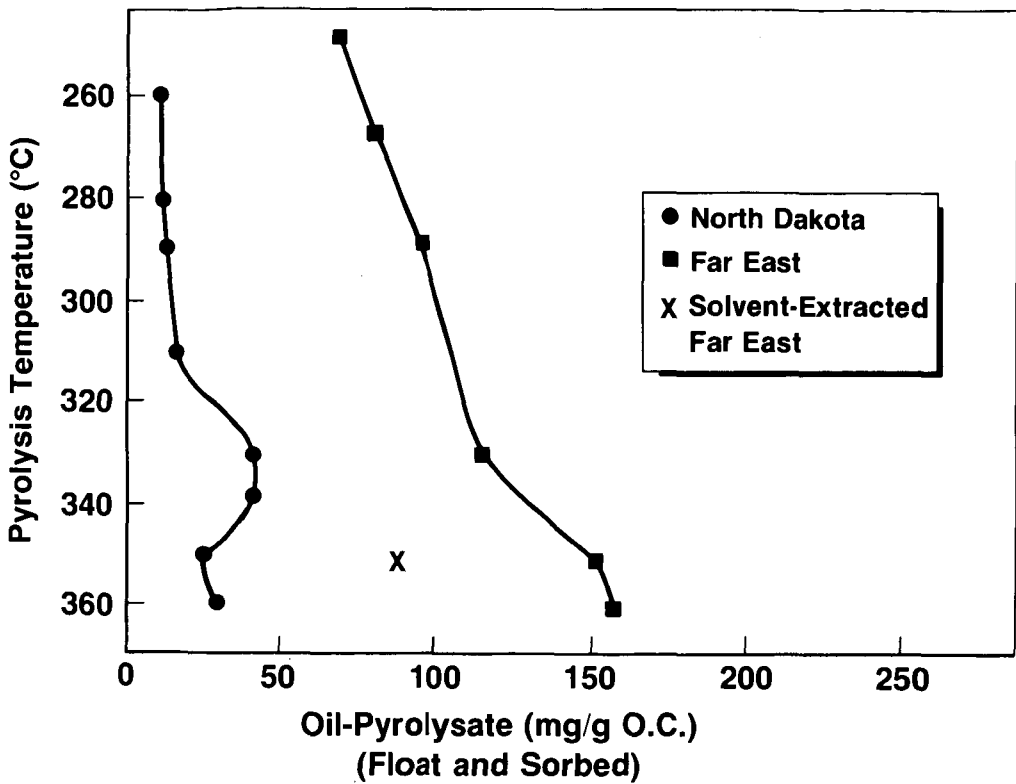
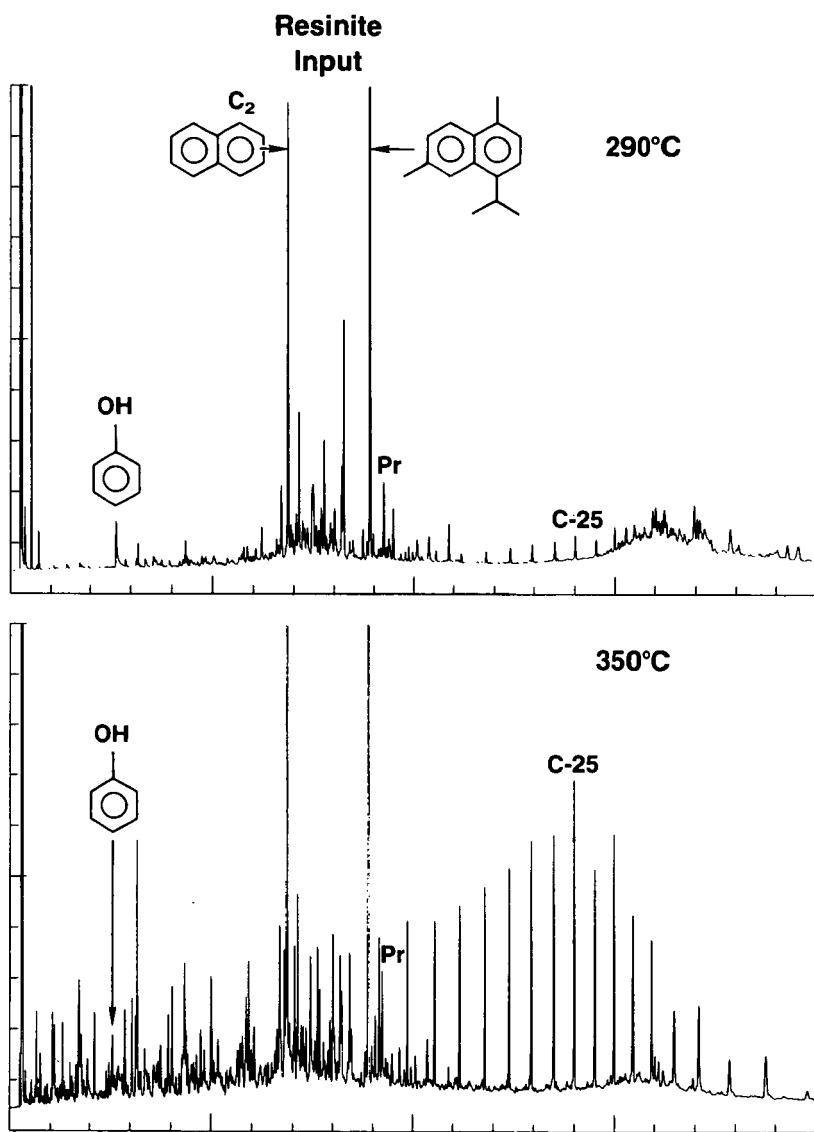


Figure 1

Oil-Pyrollysate from Hydrous Pyrolysis Experiments of Far East and North Dakota Lignites



**Figure 2**  
**Comparison of Far East Lignite Oil-Pyrolsates, 290° and 350°C**

LE 88-05126

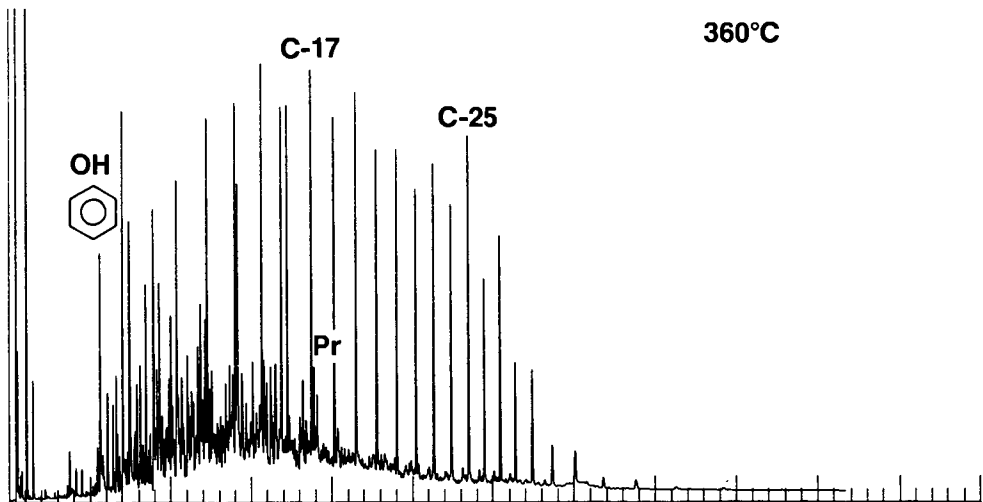
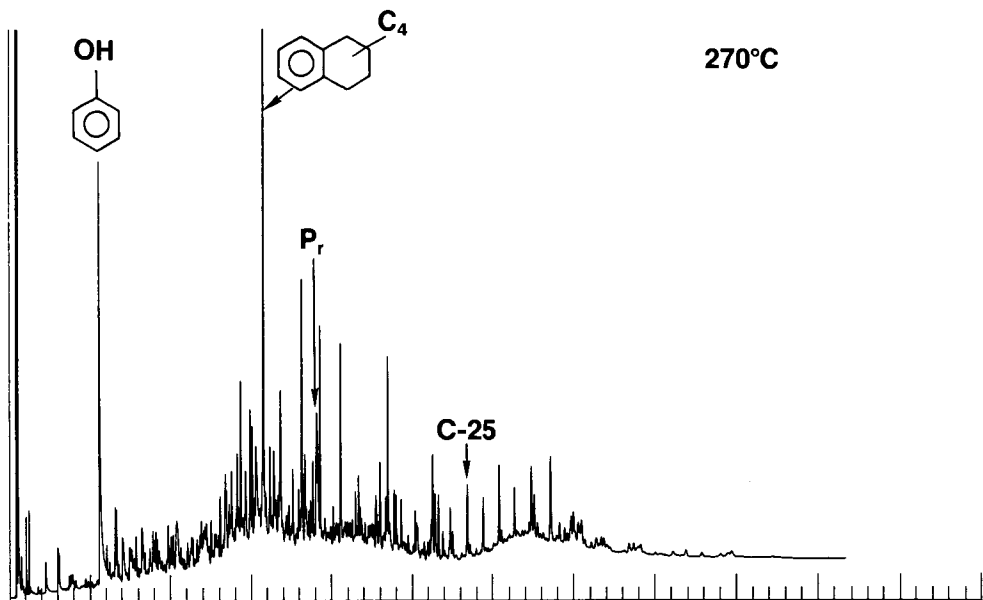


**Figure 3**  
**Comparison of North Dakota Oil-Pyrolysates, 270° and 360°C**

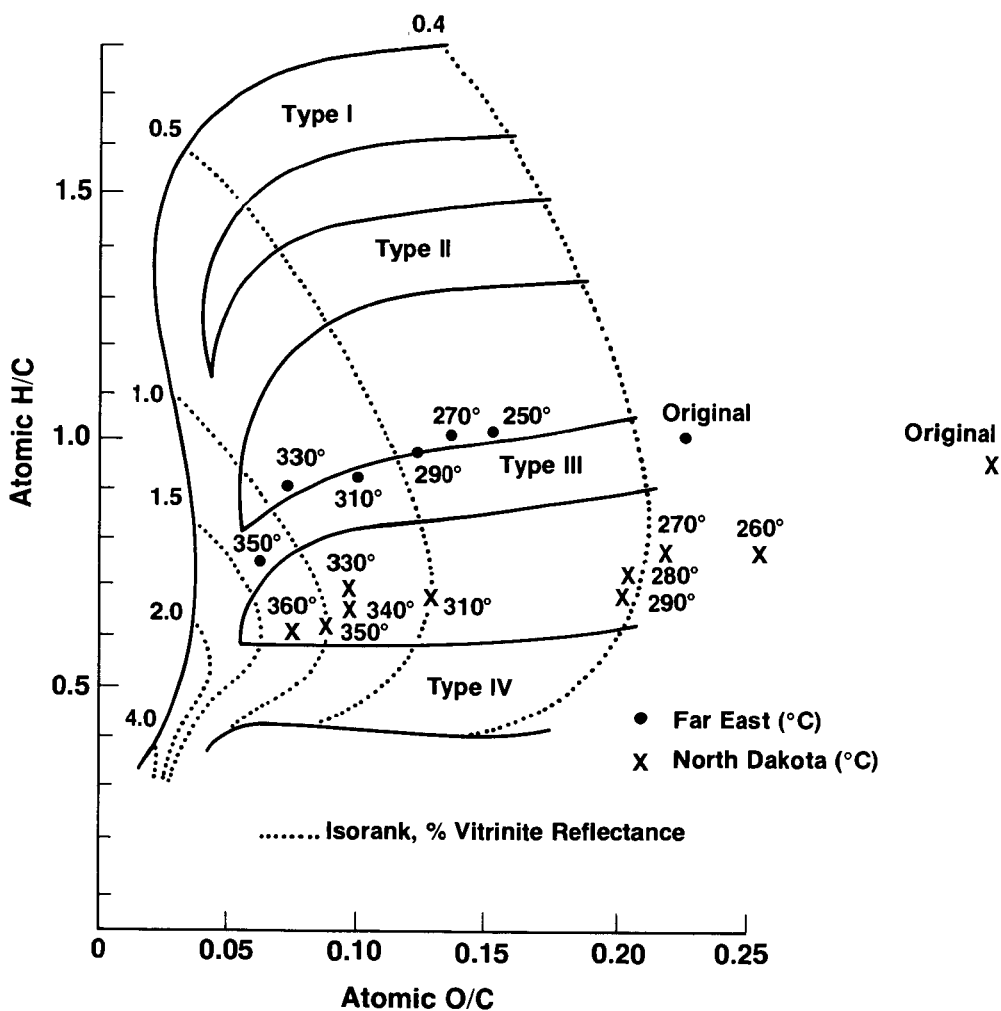


**Figure 4**  
**Atomic H/C and O/C Ratios of Far East and North Dakota Lignites from Hydrus Pyrolysis Experiments**

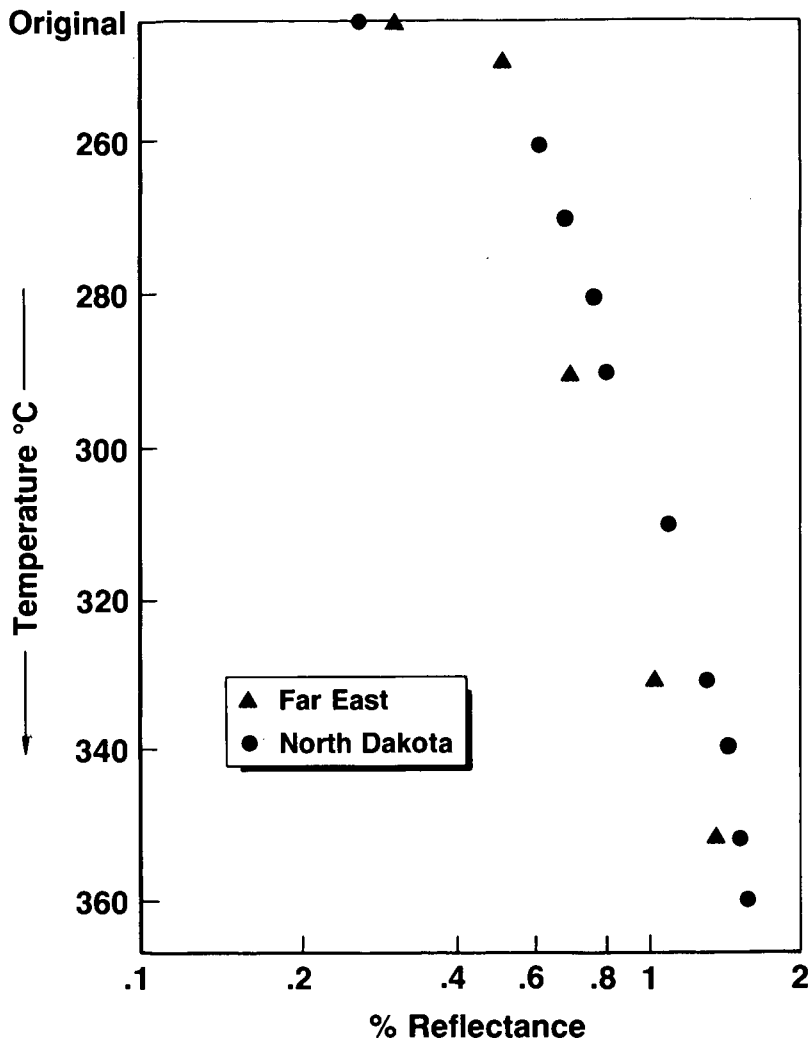


Figure 5

Vitrinite Reflectance for Far East and North Dakota Lignites Versus Hydrous Pyrolysis Temperature

LE 88-05129

CO HYDROGENATION AND OXYGENATE FORMATION OVER RUTHENIUM SUPPORTED  
ON A BASIC LAYERED DOUBLE HYDROXIDE

M. Rameswaran, Emmanuel Dimotakis and Thomas J. Pinnavaia\*

Department of Chemistry and  
Center for Fundamental Materials Research  
Michigan State University, East Lansing, Michigan 48824

**ABSTRACT**

Synthetic layered double hydroxides (LDH) such as hydrotalcite (HT),  $[\text{Mg}_6\text{Al}_2(\text{OH})_{16}](\text{CO}_3)_4 \cdot 4 \text{H}_2\text{O}$ , provide a highly basic ( $\text{pK}_a < 35$ ) environment for supporting transition metals. Ruthenium was grafted onto a HT using  $\text{Ru}_3(\text{CO})_{12}$  as a precursor and was subsequently reduced under flowing  $\text{H}_2$  at  $275^\circ\text{C}$  to ruthenium metal. The supported catalyst exhibited substantial selectivity at  $275^\circ\text{C}$  for  $\text{C}_1\text{-C}_4$  alcohols at moderately low pressures (0-190 psig). Methanol was the most dominant oxygenated product. The factors effecting the thermal stability and selectivity properties of this new class of catalyst system are presented.

**INTRODUCTION**

Layered double hydroxides, such as hydrotalcite  $[\text{Mg}_6\text{Al}_2(\text{OH})_{16}](\text{CO}_3)_4 \cdot 4 \text{H}_2\text{O}$  (HT, 3:1 Mg:Al), are anionic clay minerals. These compounds have a brucite-like structure, with positively charged hydroxide layers of aluminum and magnesium. The positive charge is compensated by intercalated carbonate anions along with some water molecules. The thermal decomposition of this material has been investigated by several laboratories [1-3]. These earlier studies indicate that the interstitial water is reversibly lost up to  $200^\circ\text{C}$ . Between  $250^\circ\text{C}$ - $450^\circ\text{C}$ , the loss of water was accompanied by dehydroxylation. Reichle [3] has reported that only above  $275^\circ\text{C}$  the formation of MgO phase along with HT phase was observed by X-ray diffraction (XRD). Beyond  $550^\circ\text{C}$  the HT phase was irreversibly lost.

Giannelis et al. [4] have grafted metal carbonyl complexes onto the pillars within the galleries of aluminum pillared montmorillonite (APM) clays. They reported that  $\text{Ru}_3(\text{Co})_{12}$  is more easily transformed into partially oxidized grafted species, even in the absence of air, when compared with other carbonyl complexes. Giannelis and Pinnavaia [5] further extended their studies to include the grafting of Rh and Pt carbonyls to the surfaces of HT. In the present study we show that it is possible to graft these carbonyl complexes onto HT.

\*To whom inquiries should be addressed.

Bulk Ru is known to be one of the most active syngas conversion catalyst with almost 100% selective to straight chain hydrocarbon [6,7]. However, the acid-base properties of the support are known to effect the selectivity of Group VIII transition metals. Thus, hydrotalcite provided us with an ideal opportunity to investigate the behavior of  $\text{Ru}_3(\text{CO})_{12}$  and Ru on a very basic oxide surface.

## EXPERIMENTAL

### HYDROTALCITE PREPARATION

A solution of 51.2g (0.20 mols)  $\text{Mg}(\text{NO}_3)_2 \cdot 6\text{H}_2\text{O}$  and 24.8g (0.067 mols)  $\text{Al}(\text{NO}_3)_3 \cdot 9\text{H}_2\text{O}$  in 200 ml of water was added drop wise to a solution of 25g (0.20 mols)  $\text{Na}_2\text{CO}_3 \cdot \text{H}_2\text{O}$  and 28g (0.70 mols) NaOH in 200 ml of water. The addition was stopped when the pH of the solution reached 10. This process, which took about 4h, was carried out with vigorous agitation. The resulting heavy slurry was refluxed at  $65 \pm 5^\circ\text{C}$  for 16h with continuous mixing. Upon cooling, the slurry was washed and centrifuged several times until almost all the salt was recovered. The slurry was then dried in air on a large glass plate [8]. The X-ray pattern indicated a  $d_{001}$  spacing of  $7.76\text{\AA}$ , which is indicative of HT with 3:1 Mg:Al. The thermal stability of the HT thus prepared was analyzed using a CAHN TGA 121 thermo-gravimetric analyzer from 25 to  $1000^\circ\text{C}$  at a heating rate of  $5^\circ\text{C}/\text{min}$ . The weight loss under isothermal conditions at  $275^\circ\text{C}$  also was investigated. The isothermal temperature was achieved using the same heating rate indicated earlier.

### RUTHENIUM IMPREGNATION

One gram of HT was evacuated at room temperature for 4h. To this HT was added to 45mg of  $\text{Ru}_3(\text{CO})_{12}$  dissolved in 100 ml of degassed  $\text{CH}_2\text{Cl}_2$ . The slurry was stirred for 20h, filtered in air, and washed with a small amount (~20 ml) of  $\text{CH}_2\text{Cl}_2$ . The percentage of Ru impregnated was determined by atomic adsorption (Galbraith Laboratory) and was found to be 0.34%. A 3.0% mixture of Ru-HT catalyst and KBr was pelletized. The IR spectrum was recorded on an IBM Model IR/44 FTIR spectrometer.

### CO-HYDROGENATION

About 0.5g of Ru-HT catalyst was loaded into a 1/4" OD, 316 stainless steel, tubular, single pass reactor. The catalyst sample was reduced in flowing hydrogen (Matheson, UHP) at  $275^\circ\text{C}$  for 6h. The reduction temperature was achieved at a heating rate of  $5^\circ\text{C}/\text{min}$ . The CO hydrogenation reaction was carried out between  $225\text{--}275^\circ\text{C}$ , and from atmospheric pressure to 190 psig at a conversion of less than 5%, in order to avoid mass and heat transfer limitations. A  $\text{H}_2/\text{CO}$  flow ratio of 2.0 was maintained

using mass flow controllers. The incoming gases were further purified by passing through a manganese/silica [9] oxygen scrubber, Linde 4Å molecular sieve to remove water and through an Al<sub>2</sub>O<sub>3</sub> trap maintained at 200 K to remove metal carbonyls. The reactor effluent was transferred through a heated line to a Hewlett-Packard 5890A GC equipped with automatic gas sampling valve and flame ionization detector. The hydrocarbons were separated using a 60m-long, 0.25 mm dia, 1µm-thick SP2100™ coated, fused silica capillary column.

## RESULTS AND DISCUSSIONS

The thermogram presented in Figure 1 for Mg<sub>6</sub>Al<sub>2</sub>(OH)<sub>16</sub>.CO<sub>3</sub>.4H<sub>2</sub>O exhibits four distinct regions, in agreement with the observations of Reichle [3]. The first region (25°-250°C) was attributed to the loss of interstitial water. At the second region (250°-325°C) the loss of water is accompanied by slow dehydroxylation. In the third (325°-500°C), rapid dehydroxylation and loss of carbonate are accompanied by HT phase transformation to mixed metal oxides. In the final region (>500°C), a stable mixed-oxide phase is irreversibly formed. According to Reichle [3], the highest temperature at which the HT phase was stable is 275°C. Therefore, we investigated the thermal stability of HT at 275°C temperature for 4h. As seen in Figure 2, there was no loss in weight after reaching 275°C over 4h period. A similar thermal treatment at 350°C resulted in a significant loss of weight even at the isothermal condition. Therefore, we used 275°C as the reduction temperature for ruthenium and the highest reaction temperature for CO hydrogenation.

The FTIR spectrum for the Ru<sub>3</sub>(CO)<sub>12</sub>-HT impregnation product is presented in Figure 3. The two peaks at 2047 and 1965 cm<sup>-1</sup> were assigned to a mononuclear [Ru(CO)<sub>x</sub>(OM≡)<sub>2</sub>]<sub>n</sub>, grafted species [4,5,10]. In this case M is either Al or Mg ions. The degradation of the neutral metal cluster carbonyl, due to their reaction with surface hydroxyl groups, results in the formation of partially oxidized grafted species on the surface of HT. Analogous species osmium complex were known to form on bulk silica and alumina supports [11-13].

The selectivity of the hydrogen-reduced Ru-HT catalyst for various hydrocarbon at 275°C at pressures ranging from 0-190 psig is tabulated in Table 1. The production of methane decreased while the total alcohol synthesis increased with increasing pressure. An opposite trend was observed with increasing temperature (Table 2). That is, the methane production increased while the alcohol production decreased when the temperature was raised from 260 to 275°C at a constant pressures of 120 psig. The percentage of various alcohols produced are presented in Table 3 as a function of pressure at 275°C. In Table 4 the selectivity is presented as a function of temperature at a constant pressure of 120 psig. It is interesting to note that

the methanol fraction is independent of pressure, but it increases with increasing temperature at constant pressure.

Metals such as Pt, Pd and Ir are known to non-dissociatively adsorb CO even at high temperature and to produce methanol almost exclusively [14]. Katzer et al [14] observed that the methanol production was related to the concentration of non-dissociatively adsorbed CO. Rhodium, however, is selective to both alcohols and hydrocarbons, depending on the nature of the material that supports it [15-17]. Rh supported on MgO is more selective towards MeOH, but when supported on a non-basic material, it is selective to hydrocarbons.

Ruthenium is known to dissociate CO at reaction temperatures and to produce mainly hydrocarbons. There are a few exceptions, of course. Some workers [18,19] have reported about 20% selectivity to alcohols for alkali promoted Ru and for Ru on MgO catalysts at pressure of 300-1000 psig. It appears that the basic environment of the Ru is responsible for such high selectivity for alcohols. The selectivity toward alcohols for the Ru-HT observed in this study is comparable to that for Ru on MgO or alkali-promoted Ru catalysts [18,19]. It is particularly noteworthy, however, that the reaction pressure employed in this study was far less than the others.

Since HT is an extremely basic material, it appears that it has altered the characteristics of Ru metal by limiting the dissociation of CO. The lower methane production and higher alcohol yield (in particular, the higher MeOH yield) at lower temperature supports this hypothesis. At higher temperatures, the CO disassociation is increased and thus the methanation reaction is promoted; at the same time, the lower concentration of undissociated CO reduces the selectivity of alcohols.

#### SUMMARY

Our results clearly demonstrate that the support material can alter the CO hydrogenation selectivity of ruthenium. This metal typically is highly selective to straight-chain hydrocarbons, but the selectivity at relatively low reaction pressures has been altered by the presence of a basic support to produce alcohols. In fact, the alcohol selectivities reported here for Ru have not been achieved at such low pressures previously.

#### ACKNOWLEDGEMENTS

The National Science Foundation Division of Materials Research (DMR-8514154), and the Michigan State University Center for Fundamental Materials Research are gratefully acknowledged for their financial support of this research.

#### LIST OF REFERENCES

1. Miyata, S., *Clays and clay Miner.*, **23**, 369 (1975).
2. Rouxhet, P. G. and Taylor, H. F. W., *Chima.*, **23**, 480 (1969).
3. Reichle, W. T., Kang, S. Y. and Eherhardt, D. S., *J. Catal.*, **101**, 352 (1986).
4. Giannelis, E. P. and Pinnavaia, T. J., *J. Am. Chem. Soc.*, in press.
5. Giannelis, E. P., Rightor, E. G. and Pinnavaia, T. J., *J. Am. Chem. Soc.*, in press.
6. Vannice., M. A., *Catal. Rev.-Sci., Eng.*, **14(2)**, 153 (1976).
7. King, D. L., *J. Catal.*, **15**, 38 (1976).
8. Reichle, W. T., *J. Catal.*, **94**, 547 (1985).
9. McIlurick, C. R. and Phillips, C. S. G., *J. Phys. E.*, **6**, 1973 (1983).
10. Kuznetsov, V. L., Bell, A. T. and Yermakov, Y. I., *J. Catal.*, **65**, 374 (1980).
11. Deebe, M., Gates, B. C., *J. Catal.*, **67**, 337 (1981).
12. Psaro, R., Ugo, R., Zanderrighi, G. M., Besson, B., Smith, A. K. and Basset, J. M., *J. Organometal. Chem.*, **13**, 215 (1981).
13. Crawford, J. E., Melson, G. A., Makovsky, L. E. and Brown, F. R., *J. Catal.*, **83**, 454 (1983).
14. Katzer, J. R., Sleight, A. W., Gajardo, P., Michael, J. B., Gleason, E. F. and McMillan, S., *Faraday Disc. Chem. Soc.*, **72**, 121 (1981).
15. Sexton, B. A. and Somorjai, G. A., *J. Catal.*, **46**, 167 (1977).
16. van Der Lee, G., Schuller, B., Post, H., Favre, T. L. F. and Ponec, V., *J. Catal.*, **98**, 522 (1986).
17. Ichikawa, M., *Bull. Chem. Soc. Jap.*, **51(8)**, 2268 (1978).
18. Bossi, A., Garbassi, F. and Petrinni, G., "Preprints of 7th Int. Cong. Catal.", Tokyo, E4 (1980).
19. Pierantozzi, R., Valagene, E. G., Nordquist, A. F. and Dyer, P. N., *J. Molec. Catal.*, **21**, 189 (1983).

Table 1

CO Hydrogenation Selectivity of Ru/HT at Various Pressures  
(275°C)<sup>a</sup>

Pressure (psig)	Hydrocarbon and Total Alcohol Yields, Wt %							
	C <sub>1</sub>	C <sub>2</sub>	C <sub>3</sub>	C <sub>4</sub>	C <sub>5</sub>	C <sub>6</sub>	C <sub>7+</sub>	ALC
0	85.5	8.8	5.7	tr				0.0
70	65.2	8.3	7.0	4.5	2.8	1.0	0.9	10.0
120	63.5	7.5	7.4	4.5	2.4	1.1	0.4	13.2
170	54.1	7.6	9.1	6.0	3.3	1.5	1.0	17.6
190	56.7	8.0	9.7	6.1	3.5	2.4	0.7	21.8

<sup>a</sup>H<sub>2</sub>/CO = 2, Conv<5%, GHSV = 1000 to 3000 h<sup>-1</sup>, ~ 0.5g of catalyst.  
Time on stream >24h.

Table 2

CO Hydrogenation Selectivity of Ru/HT at Constant Pressure  
(120 psig)<sup>a</sup>

Temp. (°C)	Hydrocarbon and Total Alcohol Yields, Wt %							
	C <sub>1</sub>	C <sub>2</sub>	C <sub>3</sub>	C <sub>4</sub>	C <sub>5</sub>	C <sub>6</sub>	C <sub>7+</sub>	ALC
260	48.0	7.0	9.3	6.7	4.0	3.5	tr	20.8
275	63.5	7.5	7.4	4.5	2.4	1.1	0.4	13.2

<sup>a</sup>H<sub>2</sub>/CO = 2, Conv<5%, GHSV = 1000 to 3000 h<sup>-1</sup>, ~ 0.5g of catalyst.  
Time on stream >24h.

Table 3

C<sub>1</sub>-C<sub>4</sub> Alcohol Distribution in the Total Alcohol Product Stream  
for Ru/HT at 275°C<sup>a</sup>

Pressure (psig)	MeOH	EtOH	PrOH	BuOH
0	0	0	0	0
70	78	22	0	0
120	75	20	5	0
170	78	18	4	0
190	74	17	4	4

<sup>a</sup>H<sub>2</sub>/CO = 2, Conv<5%, GHSV = 1000 to 3000 h<sup>-1</sup>, ~ 0.5g of catalyst.  
Time on stream >24h.

Table 4

C<sub>1</sub>-C<sub>3</sub> Alcohol Distribution in the Total Alcohol Product Stream  
for Ru/HT at 120 psig<sup>a</sup>

Temperature (°C)	MeOH	EtOH	PrOH
260	81	13	6
275	75	18	4

<sup>a</sup>H<sub>2</sub>/CO = 2, Conv<5%, GHSV = 1000 to 3000 h<sup>-1</sup>, ~ 0.5g of catalyst.  
Time on stream >24h.

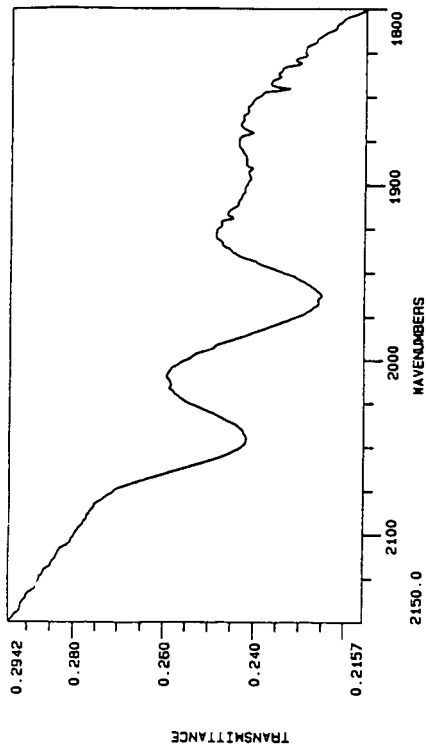


Figure 1 FTIR spectrum of the reaction product obtained from the "impregnation" of  $\text{Ru}_3(\text{CO})_{12}$  on HT. The two major peaks at 2047 and 1965  $\text{cm}^{-1}$  indicate the presence of grafted  $\text{Ru}(\text{CO})_x(\text{OH})_n$ .

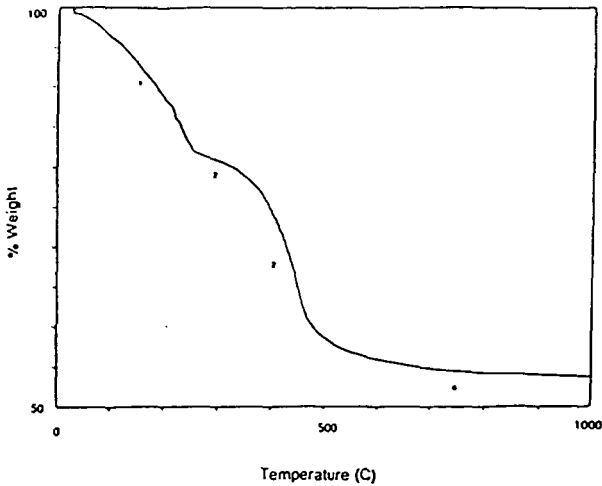


Figure 2 Thermogravimetric analysis of HT. The heating rate was 5°C/min. The four (1-4) regions are discussed in the text

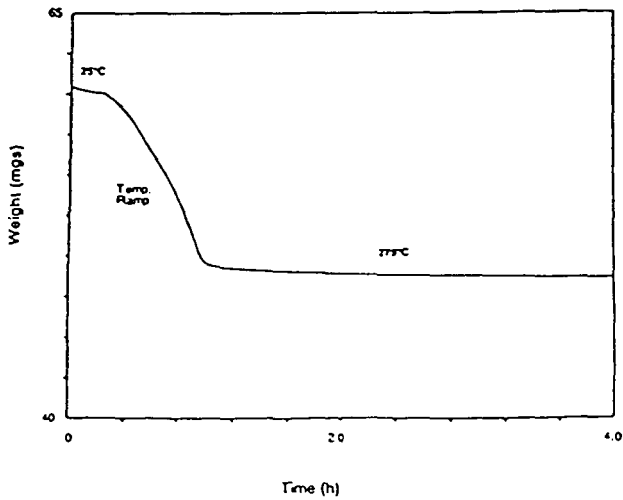


Figure 3. Thermogram of HT. Heating from 25° to 275°C was achieved using a temperature ramp of 5°C/min.

## THE EFFECTS OF PYROLYSIS CONDITIONS ON THE MACROPORE STRUCTURE OF COAL CHARs

Kyriacos Zygourakis  
Department of Chemical Engineering  
Rice University  
Houston, TX 77251-1892

### INTRODUCTION

Pyrolysis is the first stage of direct coal utilization processes. As coal particles are heated in a reactor, they release most of their volatile constituents in the form of gases and tars. The chemical transformations characterizing the pyrolysis stage are accompanied by complex morphological transformations that determine the pore structure and, consequently, the reactivity of the produced chars during the subsequent combustion or gasification stage. Gasification processes are usually diffusion-limited since the various heterogeneous reactions take place at elevated temperatures. Low utilization of the surface area associated with the micropores present in chars is expected under such conditions. Reactions occur mostly in the larger macropores that are close to the particle exterior and pore accessibility to reactants becomes a major factor in determining gasification rates. Initially, internal pores may be inaccessible to reactants. As the reaction proceeds, however, walls of closed pores will burn away exposing surface area previously unavailable for reaction and leading to substantial particle fragmentation. The opening of closed porosity, the formation of a progressively more tortuous particle exterior and the fragmentation of the original particles can lead to large enhancements of the observed gasification rates.

The major factors affecting the macropore structure of chars are the rank of the parent coals and the pyrolysis conditions. Coals can be broadly categorized as plastic or non-plastic according to their behavior during pyrolysis. Plastic coals soften as they are heated up and behave as highly viscous non-newtonian fluids over a broad temperature range. Three phases are found to coexist during this plasticity stage: a viscous (but optically isotropic) coal melt, an anisotropic liquid crystalline phase and a gaseous phase. The volatile gases form bubbles that grow and coalesce swelling the coal particles and leading to the formation of highly cellular internal pore structures that are characteristic of chars derived from plastic coals. Non-plastic coals, on the other hand, do not soften and do not undergo drastic macropore structure transformations during the pyrolysis stage. Bituminous and subbituminous coals are generally considered to be plastic, while lignites and other low rank coals belong to the non-plastic category.

The operating conditions influencing most strongly the pyrolysis process are the heating rate, the particle size and the pressure. Existing literature data offer little quantitative information on the effect of operating conditions on macropore structures, since the majority of past studies have concentrated on studying the kinetics of pyrolysis reactions and the distributions of the obtained products. Previous studies (Howard, 1981; Oh et al., 1984), however, indicate that the kinetic and transport processes occurring during pyrolysis (such as the rate of volatile release, the diffusion of volatiles into the bubbles, the transport of volatiles to the particle exterior etc.) will be governed by the time-temperature history of the coal particles. Hence, the pyrolysis heating rate is expected to have the strongest effect on the macropore structure of the chars (Hamilton, 1981).

### EFFECTS OF PYROLYSIS HEATING RATE ON MACROPORE STRUCTURE OF CHARs

A plastic coal (Illinois #6) was studied first. Coal particles in the 50-60 mesh (250-300  $\mu\text{m}$ ) range were pyrolyzed in a captive sample microreactor at five different heating rates: 0.1, 1.0, 10, 100 and 1000  $^{\circ}\text{C/s}$ . Char particles

collected from ten runs at each set of conditions were embedded in an epoxy-resin block, and one side of the block was polished to reveal random cross-sections. Digitized images for 50 particle sections were acquired from each block and they were analyzed with the digital image processor to obtain the size distribution of the two-dimensional macropore profiles. Fig. 1 presents binary images of representative cross-sections of char particles produced at the various heating rates. The black areas of these images correspond to the char matrix, while the internal white areas are the cross-sectional profiles of macropores.

The lowest heating rate (0.1 °C/s) produced char particles exhibiting a few scattered large cavities with thick walls and several smaller cavities. This is consistent with the accepted pyrolysis mechanism involving formation and growth of volatile gas bubbles. Note that most of the particles shown in Fig. 1A have retained their angular shape and only a few cenospheres were observed. Calculations indicated a moderate pressure buildup in the particle interior, since the volatile production rates are slow enough to let the gas escape before the bubbles can grow to a large size. At faster heating rates, however, the volatile production rates increase substantially leading to considerably higher pressures in the particle interior and, thus, to larger bubble sizes and more particle swelling. At a heating rate of 1 °C/s, the formation of several thin-walled cavities was observed (Fig. 1B) and several pyrolyzed char particles started exhibiting a distinct cellular internal structure. At still higher heating rates, the cellular internal structure was dominant. Chars pyrolyzed at 100 and 1000 °C/s showed exclusively thin-walled cellular structures with a few large cavities and a group of smaller secondary vesicles formed in the thin walls of the larger ones. One should note also that large particle swelling occurs at the higher heating rates leading to particles with very high porosity.

Table I summarizes the basic stereological properties for the five Illinois #6 chars. Estimates of the macroporosity  $\epsilon$  can be obtained (Weibel, 1980) from the two-dimensional particle cross-sections using the formula  $\epsilon = A_a/A_c$ , where  $A_a$  is the total area of pore profiles and  $A_c$  is the total area of the char particle sections. An estimator of the macropore surface density  $S_v$  (in (cm<sup>2</sup> pore surface)/(cm<sup>3</sup> particle)) is given (Weibel, 1980) by  $S_a = B_a/A_c$ , where  $B_a$  is the total pore profile boundary length and  $A_c$  is the total area of particle cross-sections. Both  $\epsilon$  and  $S_v$  can be estimated from two-dimensional sections without any restricting assumptions concerning the geometrical shape of the pores (DeHoff, 1983). We have also obtained the macropore volume distributions, but these measurements were based on the assumption that the macropores can be modeled as non-overlapping spheres with randomly distributed radius.

Increasing heating rates produced chars with consistently higher porosity and maximum pore radius. The increase in porosity, however, tends to level off at the higher heating rates. An increase in the macropore surface area density  $S_v$  was observed as the pyrolysis heating rate increased from 0.1 to 10 °C/s. However,  $S_v$  decreased at higher heating rates due to the appearance of very large pore cavities in the highly-swollen char particles (see Figs. 1D and 1E). The property of interest for reaction engineering calculations, however, is the specific macropore surface area  $S_g$  expressed in (cm<sup>2</sup> pore surface)/(cm<sup>3</sup> solid char). Table I shows that  $S_g$  increased dramatically with increasing heating rates. This is an indication that Illinois #6 chars produced at high pyrolysis heating rates will be more reactive at elevated temperatures where low utilization of the micropores is expected.

Pyrolysis heating rates had a much smaller effect on the macropore structure of chars produced from a non-plastic lignite coal (Wilcox, Texas). Earlier indirect measurements have indicated that the initial macropore network of non-plastic (low rank) coals remains essentially intact during pyrolysis (Gavalas and Wilks, 1980). In order to study the effect of pyrolysis heating rate on the lignite char structure, coal particles in the the 50-60 mesh size range were pyrolyzed in our microreactor at three heating rates (0.1, 10 and 1000 °C/s). Fig. 2 shows

representative images of the polished char sections taken for each sample. In contrast to the Illinois#6 chars, the cross-sections of lignite char particles show almost no visible change as the heating rate is increased. A comparison of particle sections obtained from the pyrolyzed chars and the parent coal revealed that several large fractures and cracks were formed during the pyrolysis stage. Table II presents the basic structural properties for the lignite chars. These stereological measurements show small effects of the pyrolysis heating rate both on the particle porosity and on the specific macropore surface area  $S_g$  of the char samples.

#### EFFECTS OF COAL PARTICLE SIZE ON MACROPORE STRUCTURE OF CHARS

Heat transfer in pyrolyzing coal particles can be significantly affected by the particle size. If external heat transfer controls the pyrolysis process, particle temperature will remain constant during heatup and the heating rate will decrease with increasing particle size. On the other hand, if the rate of external heat transfer is high enough, high heating rates and large particle sizes can lead to significant temperature gradients within the particle. Under such conditions, the pyrolysis reaction rates will vary significantly inside the particles.

In order to quantify the effects of particle size on the macropore structure of chars produced from the Illinois #6 coal, two additional size fractions of coal particles were pyrolyzed at 10 °C/s: 25-28 mesh (589-710  $\mu\text{m}$  particle diameter) and 100-120 mesh (125-149  $\mu\text{m}$  particle diameter). Thus, the mass of individual particles varied by about two orders of magnitude for the pyrolysis runs at 10 °C/s. This heating rate was selected in order to facilitate the detection of differences in the pore structure possibly caused by changes in the internal heating rate of the particles.

Fig. 3 presents representative cross-sections of char particles produced from the additional runs at 10 °C/s. A comparison of the cross-sections shown in Fig. 3 and Fig. 1C reveals very different pore structures for the three chars. For the smallest size fraction (Fig. 3A), we observe fewer pores per particle and the pore shape is rather rounded. The largest size fraction, on the other hand, exhibits numerous macropores per particle. The boundaries of the pore profiles are very tortuous and we see again the characteristic cellular pore structure with small pores embedded in the walls separating the larger cavities.

Table III summarizes the measurements for the macropore properties. The interesting result here is that the macroporosity of the particles was not affected by their size. This indicates that particle size did not affect the internal heating rate, pointing out that external heat transfer is not limiting for our pyrolysis reactor. The maximum pore radius observed fell from 284  $\mu\text{m}$  for the 25-28 mesh sample to 51  $\mu\text{m}$  for the 100-120 mesh sample. This decrease in macropore size was accompanied by an increase in the specific surface area of macropores per unit volume of char particle.

It must be noted here that maceral segregation may complicate the determination of particle size effects on the macropore structure of chars produced from plastic coals. Due to differences in the mechanical properties of the various coal macerals, grinding and sifting procedures may lead to enrichment of certain macerals in certain size fractions (i.e. small size fractions may contain more exinite). Thus, the well-known differences in the plastic behavior and volatile content of coal macerals can affect the macropore structure of different size fractions.

#### MODELING OF CHAR GASIFICATION

Discrete models were developed to treat the problem of char gasification at high temperatures. Low utilization of the surface area associated with the micropores is expected under such conditions, and the accessibility and surface area of the

macropores become the dominant factors in determining the temporal evolution of reaction rates.

Our earlier discrete models (Sandmann and Zygorakis, 1986) defined the pores of a solid reactant (char) by overlapping regular geometrical entities (circles, spheres or cylinders) of a given size distribution. For example, two-dimensional simulations modeled the pore cross-sections as an assemblage of overlapping circles, grew the pores by increasing the circle diameters by a fixed amount at each time step and then determined which cells had to be changed (from char to pore) to reflect the new pore dimension. As shown in Figs. 1 through 5, however, highly irregular pore structures are observed when char particle cross-sections are viewed under the microscope.

The new discrete models are based on an erosion algorithm and they avoid the computational complexities introduced when pores of arbitrary geometry are approximated by overlapping regular geometric entities. These models again employ a computational grid to represent the reacting porous solid and the macropores. However, the initial computational grids are obtained directly from digitized images of actual particle cross-sections viewed under the microscope. These images are accurate discrete approximations of a slice of the actual reacting solid. The incorporation of sophisticated digital image processing techniques in the gasification models is perhaps the most attractive feature of the new approach. For the runs presented below, the following assumptions were made.

- Only the surface area directly accessible to reactants from the irregular particle exterior participates in the reaction. Macropores in the particle interior are not initially available for reaction. When the reaction front reaches these interior pores, however, their surface area becomes available for reaction.
- Diffusional limitations in the macropores that are open to the exterior are neglected. This assumption is not expected to lead to significant errors in model predictions for the Illinois #6 chars given the large size of their internal cavities.
- Internal pores for any cross-section do not become available for reaction due to burn-through occurring at planes above or below the studied one.

The last two assumptions have been relaxed in more recent versions of the erosion algorithm. At each simulation step, the computational grid is scanned and the surface area available for reaction is identified. A statistical method is then used to erode away a single layer of pixels corresponding to the char matrix from the exterior of the char particle (and from the exterior of all particle fragments). A 3x3 neighborhood around each char pixel is examined to determine whether or not it is on an edge boundary and should be reacted. The number of pixels reacting at each step is counted and the solid reactant conversion is calculated. This process can be repeated until a specified conversion has been achieved. Particle fragmentation can also be investigated with this model by identifying all the isolated char fragments.

Fig. 4 presents the temporal evolution of reaction rates for the four particle cross sections presented in Fig. 1A. The dimensionless rate  $R_e$  and time  $\theta$  are defined as

$$R_e = \frac{1}{m_0} \frac{dm}{dt} \Delta t \qquad \theta = \frac{t}{\Delta t} = \frac{t R_s(c, T)}{\Delta x \rho_s}$$

where  $m_0$  is the mass of unreacted char,  $(dm/dt)$  is the rate of change of the reacting char mass,  $R_s(c, T)$  is the intrinsic reaction rate per unit of surface area,  $\rho_s$  is the density of the solid,  $\Delta x$  is the pixel size of the image and  $\Delta t$  is the time required to react a layer of solid with uniform thickness equal to 1  $\mu\text{m}$ .

The erosion rate for the particle exhibiting the large cenosphere (ILL106 in Fig. 1A) decreases initially and then jumps to very high levels when the large internal cavity opens up for reaction. At this point, the cross-section fragments considerably and disappears soon thereafter. The ILL102 particle in Fig. 1A has several large cavities with thin walls separating them from the particle exterior. Thus, the erosion rates calculated for this cross-section jump to very high values as these cavities open up at fairly low conversions (less than 20%). The ILL105 cross-section of Fig. 1A, on the other hand, exhibits numerous smaller cavities that open up for reaction at different time levels giving rise to the characteristic jumps in the reaction rate observed in the experiments by Sundback et. al. (1984). In this case the reaction rates remain at relatively high levels for a large time interval. Finally, the more "solid" cross-section of Fig. 1A (ILL101) exhibits a steady decrease in erosion rate for a long period of time until the single large cavity opens up. A large jump in the erosion rate is observed at this point and the rate decreases slowly after achieving its maximum value. Another interesting observation from Fig. 4 concerns the wide range of particle burnout times predicted by the discrete simulations. These variations are clearly attributed to the large internal cavities and the different macro-properties of the individual particles.

Simulation results from runs on all particle sections can provide an indication of the expected average gasification behavior for a char sample. Fig. 5 presents the average reaction rate vs. time patterns for the three Illinois #6 chars produced by pyrolyzing coal particles of different sizes at 10 °C/s. Due to its small particle size and large external surface area, the 100-120 mesh sample exhibits a high initial rate, a sharp rate maximum and very short reaction times. As the particle size is increased, the reaction rates decrease and their burnout times increase significantly.

#### ACKNOWLEDGMENT

This work was partially supported by the Department of Energy under the contract DE-FG22-87PC79930.

#### REFERENCES

- Gavalas, G.R. and Wilks, K.A., AIChE J., 26, 201 (1980).
- Hamilton, L.H., Fuel, 60, 955 (1981).
- DeHoff, R.T., J. Microscopy, 131, 259 (1983).
- Howard, J.B., "Fundamentals of Coal Pyrolysis and Hydropyrolysis", in Chemistry of Coal Utilization, p. 665, Elliott, M.A., Ed., John Wiley (1981).
- Oh, M., Peters, W.A. and Howard, J.B., Procs. 1983 International Conference on Coal Science, p. 483, International Energy Agency (1983).
- Sandmann, C.W. and Zygourakis, K., Chem. Eng. Sci., 41, 733 (1986).
- Sundback, C.A., Beer, J.M. and Sarofim, A.F., Procs. 20th International Symposium on Combustion, p. 1495, Ann Arbor, Michigan, August 12-17 (1984).
- Weibel, E.R., "Stereological Methods", vol. 2, Academic Press (1980).

**TABLE I**  
**Macropore Structural Properties of Illinois #6 Chars**  
**Produced at Various Heating Rates**

Heating Rate	Porosity	Surface Area Density (cm <sup>2</sup> /cm <sup>3</sup> particle)	Specific Surface Area (cm <sup>2</sup> /cm <sup>3</sup> solid)	Maximum Pore Radius (μm)
0.1	0.356	527	822	135
1.	0.526	759	1,599	173
10.	0.709	908	3,116	153
100.	0.795	700	3,409	194
1000.	0.873	695	5,470	224

**TABLE II**  
**Macropore Structural Properties of Lignite Chars**  
**Produced at Various Heating Rates**

Heating Rate	Porosity	Surface Area Density (cm <sup>2</sup> /cm <sup>3</sup> particle)	Specific Surface Area (cm <sup>2</sup> /cm <sup>3</sup> solid)	Maximum Pore Radius (μm)
0.1	0.140	1,011	1,176	31.0
10.	0.153	1,107	1,307	25.5
1000.	0.195	1,369	1,700	25.6

**TABLE III**  
**Effects of Coal Particle Size on the Macropore**  
**Structural Properties of Illinois #6 Chars**

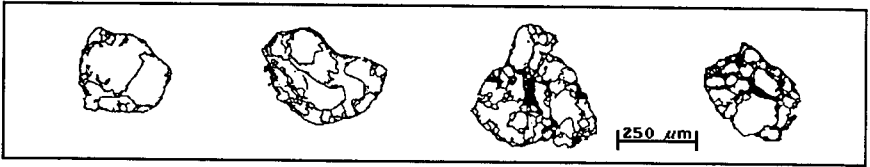
Particle Size (mesh)	Porosity	Surface Area Density (cm <sup>2</sup> /cm <sup>3</sup> particle)	Specific Surface Area (cm <sup>2</sup> /cm <sup>3</sup> solid)	Maximum Pore Radius (μm)
100-120	0.689	1,898	6,106	50.5
50- 60	0.708	908	3,116	153
25- 28	0.688	729	2,339	351



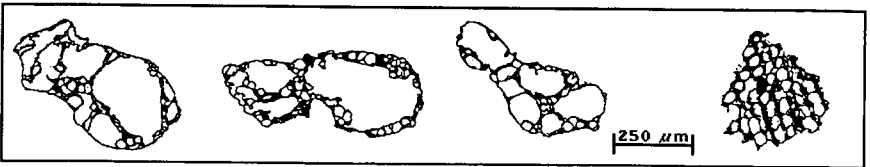
(A) 0.1 C/s



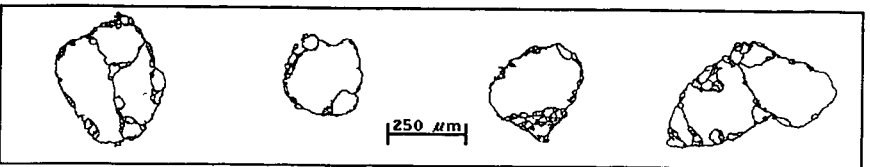
(B) 1.0 C/s



(C) 10. C/s



(D) 100. C/s



(E) 1000. C/s

Figure 1: Binary images of particle cross-sections for Illinois #6 chars produced at various pyrolysis heating rates (Coal particle size: 50-60 mesh).

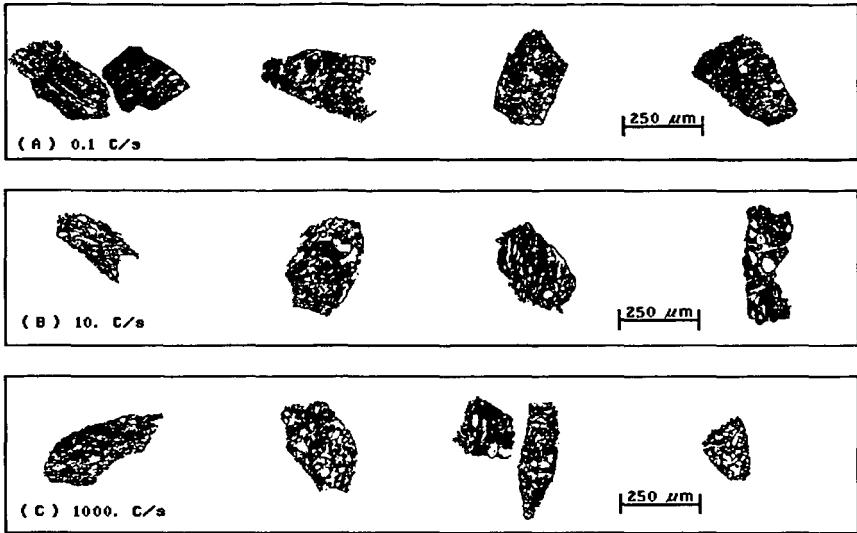


Figure 2: Binary images of particle cross-sections for lignite chars produced at various pyrolysis heating rates (Coal particle size: 50-60 mesh).

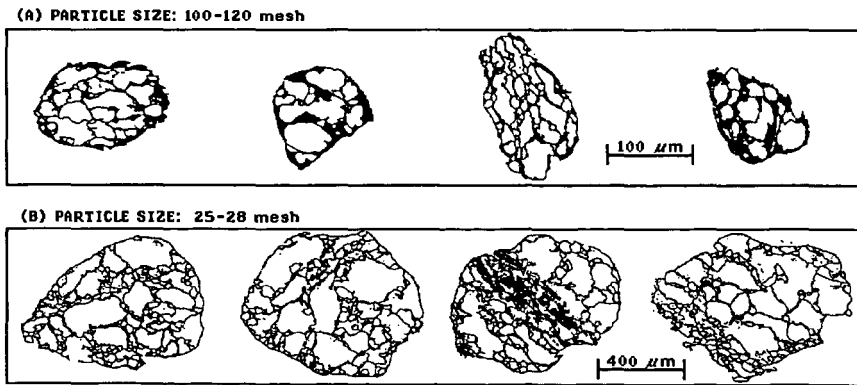


Figure 3: Binary images of particle cross-sections for Illinois #6 chars produced from different sizes of coal particles (Heating Rate: 10 °C/s).

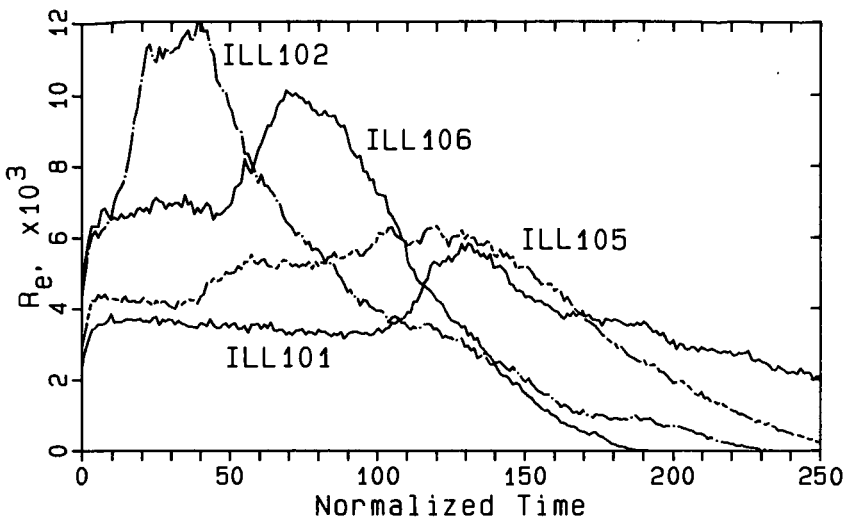


Figure 4: Temporal evolution of predicted reaction rates from four simulation runs with Illinois #6 char particles.

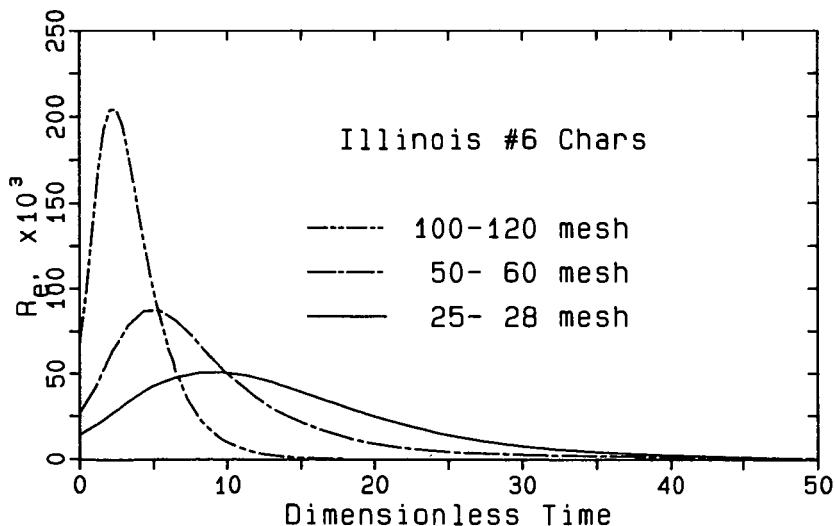


Figure 5: Effect of coal particle size on the reaction rates predicted for three Illinois #6 chars. Model predictions are averages for 48 particle cross-sections.

## THE EFFECT OF MILD OXIDATION ON THE THERMAL DESULFURIZATION AND HYDRODESULFURIZATION OF TWO ILLINOIS BITUMINOUS COALS IN A FLUIDIZED BED REACTOR

M. D. Stephenson, A. D. Williams, M. Rostam-Abadi and C. W. Kruse  
Illinois State Geological Survey  
615 East Peabody Drive  
Champaign, IL 61820

### ABSTRACT

Two high sulfur Illinois No. 6 coals were desulfurized in a fluidized bed reactor (FBR) to less than one percent sulfur by a thermal and chemical approach which included pyrolysis followed by char hydrodesulfurization. Chars were prepared for hydrodesulfurization by three different procedures; pyrolysis only, oxidation prior to pyrolysis and oxidation after pyrolysis. Pre-oxidizing conditions reduced agglomeration during pyrolysis and for one coal, which was physically cleaned, it led to significantly increased overall sulfur removal compared to the non-oxidized char. Oxidation after pyrolysis had no obvious beneficial effects. Under the best conditions tested, chars were produced having sulfur contents less than one percent for both coals.

### INTRODUCTION

Efforts to abate the deleterious impact of burning high sulfur coals are easily classified into three approaches. Post-combustion desulfurization, which includes wet limestone scrubbing, is being utilized by electric utilities but is beset by high capital and operating costs. The second category, desulfurization during combustion, includes fluidized bed combustion. This method of sulfur dioxide control is quite promising, but has not yet gained widespread usage by electric utilities. The third classification is precombustion desulfurization which includes physical and chemical coal cleaning. As yet, only physical cleaning is used commercially but it is limited to inorganic sulfur removal.

One approach to removing sulfur, including organic sulfur, is to first pyrolyze the coal and follow this step with high temperature hydrodesulfurization. This combination of steps is quite effective in removing a significant amount of the total sulfur from high sulfur coals. The products of these two steps include up to one barrel of pyrolysis oil per ton of coal, a low to medium Btu gas, coal char and elemental sulfur [1]. The relative amounts of each product depend on the coal feed and on the conditions used for the pyrolysis and hydrodesulfurization steps.

In the work described here, two Illinois basin coals were pyrolyzed in a fluidized bed reactor under a variety of conditions and then subjected to hydrodesulfurization. Three pyrolysis treatments were employed. The first treatment, denoted as pre-oxidized, consisted of a mild oxidation prior to pyrolysis, followed by pyrolysis under nitrogen. The second treatment, denoted as non-oxidized, was pyrolysis under a nitrogen atmosphere. The third treatment, denoted as post-oxidized was identical to the second or non-oxidized treatment, except that a mild oxidation occurred after the pyrolysis step. Thus, three chars were produced, pre-oxidized, non-oxidized, and post-oxidized, and these were used as hydrodesulfurization feeds.

While preoxidation is effective in decaking highly agglomerating coals [2], it does lower the yield of pyrolysis oil and is undesirable for this reason alone. However, preoxidation apparently leads to larger pores in an otherwise microporous char [3]. This tends to increase both the rate and the extent of hydrodesulfurization [4]. Since pre-oxidation has been effective in producing chars which are more reactive towards hydrogen, it was hypothesized that an oxidation of the char after removal of the volatile matter might also be effective. This processing sequence would permit maximum conversion of coal to pyrolysis oil. Agglomeration would be averted in some other way such as multistaged heating.

## EXPERIMENTAL

Coal samples - Two Illinois No. 6 coals were used in this study. The samples were obtained from the Illinois Basin Coal Sample Program (IBCSP) and are referred to as the IBCSP-1 and IBCSP-4 samples [5]. The IBCSP-1 coal is a mine-washed sample containing 4.62% total sulfur of which 3.35% is organic sulfur. The IBCSP-4 sample is a Run-of-Mine sample containing 34% ash and 4.2% total sulfur (equivalent to 9.87 lbs  $\text{SO}_2/\text{MMBtu}$ ). In order to reduce the mineral matter and pyritic sulfur content, two types of physically cleaned coal were prepared from the IBCSP-4. A "deslimed" coal was prepared by slurring and agitating the sample and then sieving it over a 235 mesh screen. The step effectively reduced the clay content of the sample, but retained much of the coarser pyrite and other mineral matter. The sample after treatment had 14.8% ash, 3.05% pyrite and 6.28% total sulfur on a dry ash free (daf) basis. A 28x200 mesh fraction was prepared from the deslimed coal utilizing a staged crushing and screening technique to ensure that the size fraction was representative of the starting material.

A second sample of physically cleaned IBCSP-4 was prepared using a gravity concentrating table in order to reject liberated coarse pyrite grains and other mineral matter. The sample was also deslimed using the above procedure to reject any clays that reported to the coal fraction. Following this treatment, the "tabled" coal had 4.18% total sulfur of which 1.22% sulfur was pyritic. Analyses of the 28x200 mesh fractions of both tabled and deslimed coal appear in Table 1.

Char production - Chars for hydrodesulfurization experiments were prepared in bulk using a 2-inch, batch, fluidized bed reactor. The description of this apparatus appears elsewhere [6]. Basically, 200-gm batches of coal were pyrolyzed in this system and when appropriate, reacted with gaseous streams of dilute oxygen. The reactor was constructed of type 304 stainless steel and was heated externally by a 3-inch, tube furnace. A microprocessor was used to control the bed temperature via a type K thermocouple immersed in the center of the bed.

The three different types of chars prepared here are designated as pre-oxidized, non-oxidized, and post-oxidized. Several batch runs at each treatment regime were necessary to provide kilogram-quantities of each type of char for hydrodesulfurization tests. After combining the appropriate batches, the chars were then riffled into 25-gm portions, and stored under inert conditions in sample bottles which were sealed with paraffin.

Pre-oxidized chars were prepared by heating a 200-gm charge of coal to 250°C in the 2-inch FBR using nitrogen as a fluidizing gas. Once at 250°C, the fluidizing gas was switched to five percent oxygen in nitrogen. The coal was fluidized under these conditions for 30 min. at which time the fluidizing gas was switched back to nitrogen. The temperature was raised to 850°C and held there for 15 min. The reactor was cooled to ambient conditions under a purge of nitrogen.

Non-oxidized chars were prepared using heating schedules similar to those used by the FMC Char Oil Energy Development (COED) process [7]. Multistaged or slow heating of our coals was necessary to avoid agglomeration. For IBCSP-4 coal, four soak temperatures were used, 350, 375, 400, and 425°C. For IBCSP-1 coal, a heating rate of 1.7°C/min was employed without any isothermal soak periods. Agglomeration did not occur. Once the temperature reached 850°C, the char was held for 15 min. before cooling to ambient conditions under a purge of nitrogen.

The post-oxidized samples were prepared in the same way as the non-oxidized samples with one exception. During the cool down period, the bed temperature was allowed to reach 450°C for IBCSP-1 coal or 250°C for IBCSP-4 coal and then held at that temperature while five percent oxygen was admitted as a fluidizing gas. The temperature was lowered to 250°C for the second coal because this temperature was preferable for a comparison of pre-oxidization with post-oxidation. The post-oxidative treatment was continued for 15 min. (IBCSP-1) or 30 min. (IBCSP-4) after which the fluidizing gas was switched back to nitrogen. The reactor was then cooled to ambient conditions.

Hydrodesulfurization - A 1-inch batch fluidized bed hydrodesulfurizer was used for char hydrodesulfurization tests. The reactor was constructed from a 24-inch length of type 446 stainless steel, schedule 40 pipe. A distributor plate of porous Hastelloy-X stainless steel (average pore size of 10 microns) was located nine inches from the bottom of the pipe. The space below the plate was filled with 1/4-inch ceramic Raschig rings which served as a gas preheater. Type 446 stainless steel caps were used at both ends of the reactor and were fitted to accept 1/4-inch tube fittings.

For each hydrodesulfurization (HDS) experiment, approximately 10 grams of char was accurately weighed and charged to the reactor. The sample was heated rapidly to the reaction temperature under a nitrogen flow which generally took about 45 min. Once the system reached the designated reaction temperature ( $\pm 1^\circ\text{C}$ ), nitrogen was shut off and hydrogen was introduced to the reactor for a period of 90 minutes except where noted. When the desired treatment time had elapsed, hydrogen was turned off and nitrogen was once again introduced to the reactor. The reactor system was allowed to cool to near room temperature and the desulfurized char was removed, weighed and analyzed.

## RESULTS AND DISCUSSION

Hydrodesulfurization of IBCSP-1 coal - Three chars were prepared from IBCSP-1 coal (pre-oxidation, non-oxidation, and post-oxidation). As shown in Figure 1, it can be seen that after pyrolysis, the post-oxidized char had the lowest sulfur content, approximately 2.4%. The non-oxidized char contained roughly 2.7% sulfur while the pre-oxidized char was marginally higher at 2.8% sulfur. Table 2 shows that hydrodesulfurized chars were produced having sulfur contents of 0.9% sulfur (an average of four combinations of temperature and hydrogen flow rate) from pre-oxidized coal compared to 1.2% average sulfur for the same array of conditions for the post-oxidized sample. By taking an average over the four sets of conditions, the effect of oxidation is measured over a wide range of conditions.

Examination of the percent initial char sulfur remaining after hydrodesulfurization reveals that hydrodesulfurization removed the most sulfur from the pre-oxidized sample. On average, only 27.4% of the sulfur initially present in the HDS sample remained after treatment. For the non-oxidized sample, 34.7%, on average, of the char's sulfur remained after hydrodesulfurization while 42.6%

remained for the post-oxidized char. Apparently, pre-oxidized chars are the most reactive towards hydrogen.

The final sulfur contents of the chars do not show appreciable differences between the treatments. Thus, there is no apparent advantage to post-oxidation as a part of a multi-step process which includes pyrolysis and hydrodesulfurization. As can be seen in Figure 1, sulfur is removed during the post-oxidation. The amount is relatively small but it is presumably converted to sulfur dioxide. Also, the amount of sulfur removed during hydrodesulfurization, the sulfur being removed as hydrogen sulfide, is the least of all three treatments. When considering product differences with regard to ease of gas cleanup, the post-oxidation treatment would be the most troublesome if it produced dilute sulfur dioxide that had to be removed from the gas stream. Mild pre-oxidation is not expected to yield appreciable sulfur dioxide. As there was no overall improvement in desulfurization when post-oxidized chars were used, this treatment was not investigated further with this particular coal.

Hydrodesulfurization of deslimed IBCSP-4 coal - As shown in Figure 2, the sulfur content of post-oxidized chars, non-oxidized chars and pre-oxidized chars produced from this coal with higher pyrite content were all similar. As shown in Table 3, all three types of hydrodesulfurized chars, on average, were similar in sulfur content. Although there is some scatter among the data, there is no treatment that is clearly superior. As with IBCSP-1, the post-oxidation treatment is of dubious merit and was not investigated further.

Pre-oxidation is quite effective in controlling agglomeration although pyrolysis oil yields are usually reduced. For the case of IBCSP-1 and IBCSP-4 (deslimed) coals, the sulfur content of the hydrodesulfurization products were not appreciably affected by pre-oxidation. However, due to its extreme effectiveness in handling caking coals, it was investigated further.

Effect of physical cleaning of IBCSP-4 coal - If a coal contains an appreciable quantity of pyritic sulfur, it is desirable to physically remove as much as possible before any processing. This is due to the thermodynamic limitations imposed by the unfavorable reaction between ferrous sulfide and hydrogen. Pyrite is converted to ferrous sulfide during pyrolysis and in order to remove this remaining inorganic sulfur, high hydrogen space velocities are required [8]. In the case of IBCSP-4, where the pyritic sulfur content was 3.05%, as compared to 1.34% pyritic sulfur in the IBCSP-1 coal, it seemed logical to remove additional pyrite by tabling. This step alone lowered the pyritic sulfur content to 1.22% or roughly that of the IBCSP-1 coal.

Removing pyritic sulfur from the tabled coal resulted in a vastly more effective hydrodesulfurization step. This is clearly demonstrated in the data shown in Table 4. Data in this table are organized in eight sets of two experiments. For each set, the only difference between the experiments is the level of physical cleaning. For the first set, lines one and two, the sulfur content in the product is 2.99% for the deslimed and 2.01% for the tabled coal. This same trend can be seen in each succeeding set of runs. On average the tabled coal resulted in a hydrodesulfurized product which was 1.25 percent lower in sulfur content.

A close inspection of the data in Table 4 reveals a synergistic effect between physical cleaning and oxidation. In lines 1 and 3, all factors remain constant except for oxidation. This is also true for lines 2 and 4, 5 and 7, 6 and 8, etc. For deslimed coal, the effect of oxidation on desulfurization is generally

quite small or nonexistent. However for tabled coal, desulfurization is significantly increased for all cases in which pre-oxidized chars were used. Thus, with this particular cleaned coal, pre-oxidation is quite effective in aiding hydrodesulfurization. The relative merit of a pre-oxidation step compared to no oxidation depends on technical and economic considerations. Pre-oxidation would permit coals to be pyrolyzed faster than by staged heating resulting in a cost savings. However, the decreased oil yields would impact negatively on the economics.

Concluding remarks - A combination of pyrolysis and char hydrodesulfurization is an effective method to reduce the total sulfur content of high sulfur coals to less than one percent. Oxidation, both before and after pyrolysis, generally had little effect on the overall level of desulfurization for two Illinois basin coals, although pre-oxidation markedly increased the extent of desulfurization for physically cleaned IBCSP-4. In fact, the only appreciably desulfurized IBCSP-4 chars had been pre-oxidized and physically cleaned.

#### REFERENCES

1. Stephenson, M. D. and C. W. Kruse, 1985, in Y. A. Attia, ed., Processing and Utilization of High sulfur coals, Coal Science and Technology 9, Elsevier, pp 373-392.
2. Boodman, M. S., T. F. Johnson and K. C. Krupinski, 1977, in T. D. Wheelock, ed., Coal desulfurization, ACS Symposium Series 64, 248-266, Washington, D.C.
3. Block, S. S., J. P. Sharp and L. J. Darlage, 1985, Fuel, 54(4), 113-119.
4. Fleming, D. K., R. Smith, and M. R. Y. Aquinio, 1977, in T. D. Wheelock, ed., Coal desulfurization, ACS Symposium Series 64, 267-279, Washington, D. C.
5. Kruse, C. W., R. D. Harvey, and D. M. Rapp, 1987, ACS Div. Fuel Chem. Pre-prints, 32(4), 359-365.
6. Stephenson, M. D. and C. Liu, Quarterly Technical Report to the Center for Research on Sulfur in Coal for the period September 1, 1986-August 31, 1987, 40 pp., 1987.
7. Paige, W. A., 1977, Energy Communications, 3(2), 127-150.
8. Stephenson, M. D., M. Rostam-Abadi, L. A. Johnson and C. W. Kruse, 1985, in Y. A. Attia, ed., Processing and Utilization of High sulfur coals, Coal Science and Technology 9, Elsevier, pp 353-372.

#### ACKNOWLEDGEMENTS

This work was funded in part by grants from the Illinois Coal Development Board through the Center for Research on Sulfur in Coal. The authors gratefully acknowledge Mr. Scott Ellis, Mr. Jeffrey Sprague, and Dr. Gary Clauson for their laboratory expertise and Mr. Dave Rapp for his assistance in preparing physically cleaned coal samples.

Table 1. Analysis of feed coals.

Analysis	IBCSP-1	IBCSP-4	IBCSP-4	
			Deslimed	Tabled
<u>Proximate, wt% as received</u>				
Moisture	14.1	10.2	3.5	1.5
Volatile matter	37.9	27.4	36.6	38.3
Fixed carbon	39.2	28.2	45.1	50.4
Ash	8.8	34.2	14.8	9.8
<u>Ultimate, wt% daf</u>				
Hydrogen	5.42	5.25	5.26	4.64
Carbon	75.41	69.86	77.91	81.66
Nitrogen	1.32	1.22	1.57	1.90
Oxygen	12.96	11.29	8.97	7.61
Sulfur	4.75	6.37	6.28	4.18
pyritic	1.34	3.54	3.05	1.22
organic	3.34	2.67	3.23	2.86
sulfatic	0.07	0.15	tr	0.10
Calorific value, Btu/lb	12,606	8,492	11,554	12,556
Specific sulfur content, lbs SO <sub>2</sub> /MMBtu	5.81	9.87	8.88	5.91

Table 2. Hydrodesulfurization of char from IBCSP-1 coal<sup>a</sup>.

Oxidation	Experimental Conditions		Sulfur in HDS char %	Initial char S left in HDS char %	
	Temp °C	Flow cc/min			
Pre	800	500	0.91	27.6	
Pre	850	500	1.00	30.5	
Pre	800	1000	0.92	28.0	
Pre	850	1000	0.83	23.3	
			Average	0.92	27.4
Non	800	500	1.33	42.9	
Non	850	500	1.13	35.2	
Non	800	1000	0.88	27.8	
Non	850	1000	1.06	32.8	
			Average	1.10	34.7
Post	800	500	1.27	47.2	
Post	850	500	1.24	43.8	
Post	800	1000	1.03	35.5	
Post	850	1000	1.24	44.0	
			Average	1.20	42.6

<sup>a</sup>Time, 90 minutes

Table 3. Hydrodesulfurization of char from deslimed IBCSP-4<sup>a</sup>.

Oxidation	Sulfur in HDS char wt %	SO <sub>2</sub> from burning HDS char lbs/MMBtu	Initial char S left in HDS char %
Pre	1.84	3.23	45.2
Pre	1.95	3.36	45.5
	Avg 1.89	3.30	45.3
Non	1.95	3.44	40.0
Non	1.67	2.80	38.4
Non	2.04	3.50	46.2
	Avg 1.89	3.25	41.5
Post	1.90	3.34	43.7
Post	2.27	3.97	52.1
	Avg 2.09	3.66	47.9

<sup>a</sup>Temperature, 850°C; time, 90 minutes; H<sub>2</sub> flow rate, 1000 cc/min.

Table 4. Hydrodesulfurization of char from tabled and deslimed IBCSP-4<sup>a</sup>.

No.	Experimental Conditions				Sulfur in HDS char wt %	SO <sub>2</sub> from burning HDS char lbs/MMBtu	Initial char S left in HDS char %
	Coal Type	Pre-Oxi- dized	Temp °C	Time min.			
1	Deslimed	No	750	45	2.99	5.25	70.05
2	Tabled	No	750	45	2.01	3.30	66.40
3	Deslimed	Yes	750	45	3.40	5.88	86.00
4	Tabled	Yes	750	45	1.50	2.42	54.30
5	Deslimed	No	850	45	2.57	4.53	59.40
6	Tabled	No	850	45	1.62	2.65	52.30
7	Deslimed	Yes	850	45	2.51	4.30	58.85
8	Tabled	Yes	850	45	1.22	1.97	43.70
9	Deslimed	No	750	90	2.77	4.88	64.55
10	Tabled	No	750	90	1.76	2.85	57.25
11	Deslimed	Yes	750	90	2.64	4.49	63.10
12	Tabled	Yes	750	90	1.14	1.82	40.95
13	Deslimed	No	850	90	2.24	3.99	51.20
14	Tabled	No	850	90	1.41	2.31	45.60
15	Deslimed	Yes	850	90	2.28	3.86	53.05
16	Tabled	Yes	850	90	0.77	1.24	27.15

<sup>a</sup>Hydrogen flow rate, 750 cc/min.

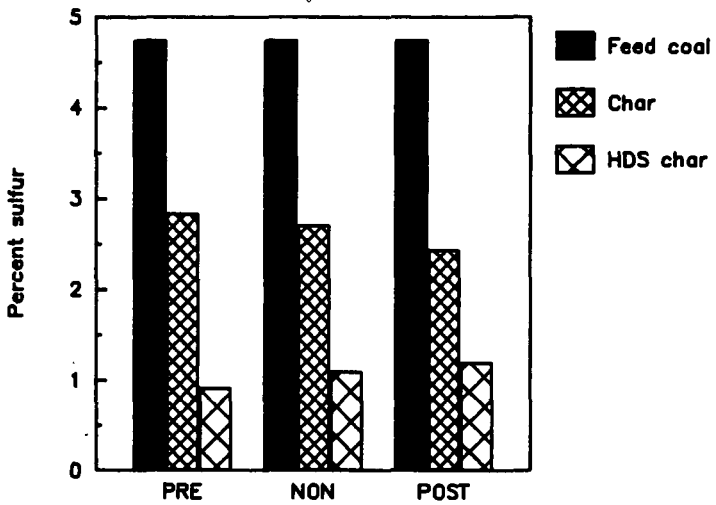


Figure 1. Desulfurization of IBCSP-1.

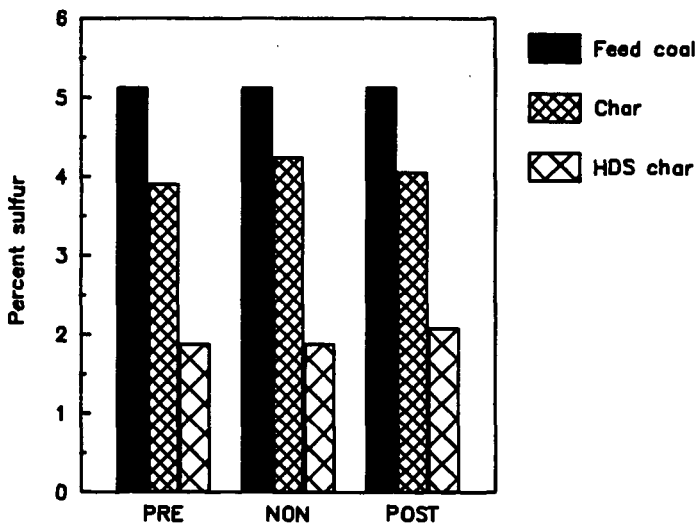


Figure 2. Desulfurization of IBCSP-4.

Coal Gel Chemistry I. An Aspect of Synergistic Effects  
on the solvent Swelling of Coal

Tetsuo Aida<sup>1</sup>, Yasuhumi Shimoura<sup>1</sup>, Nobuyuki Yamawaki<sup>1</sup>, Masayuki Fujii<sup>1</sup>  
Thomas G. Squires<sup>2</sup>, Masakuni Yoshihara<sup>3</sup>, Toshihisa Maeshima<sup>3</sup>

<sup>1</sup>Department of Industrial Chemistry, Faculty of Engineering  
Kinki University in Kyushu, 11-6 Kayanomori, Iizuka, Fukuoka 820, JAPAN

<sup>2</sup>Ames Laboratory, Iowa State University, Ames Iowa 50010, U.S.A.

<sup>3</sup>Department of Applied Chemistry, Faculty of Science & Engineering  
Kinki University, 3-4-1 Kowakae, Higashiosaka, Osaka 577, JAPAN

INTRODUCTION

For a long time, the mixed solvents, such as alcohol-benzene, are conveniently used for coal extractions(1), in which solubilities of coal products used to be enhanced to those in the individual solvents. Most recently, Iino et al. (2) reported powerful binary solvent systems for coal extractions which were composed of carbondisulfide and aprotic dipolar solvents like a DNF or N-methylpyrrolidinone. Although it has long been pointed out that there was a correlation between the increase of extractability and the increase of swelling(2, 3), the mechanism of the synergistic effect on the solvent swelling of coal has been controversial in the coal chemistry. For examples, the effects observed in the binary solvent systems composed of the amine as a counter component had been discussed by Hombach(4) and Larsen(5), based on the solubility parameters and hydrogen bondings in the coal matrix, respectively.

Meanwhile, recently, we revealed the significant steric requirement on the solvent swelling of coal(6). In the course of the further study on the solvent swelling by using various solvents we have learned that there was a curious similarity on the solvent systems adopted by previous researchers(4, 5), which were commonly composed of a sterically hindered and a less sterically hindered solvents, and also have found that the relaxation of the steric requirement of coal by the initial formation of the "Coal Gel" of a less hindered solvent would be responsible to the synergistic effect on the solvent swelling of coal.

This paper presents the results of the studies on the synergistic effects of binary solvents on the solvent swelling of coal, based on the steric requirement.

## EXPERIMENTAL

The swelling measurements were carried out as described into previous paper (7). Coal, Illinois #6 coal, used in these studies were from the Ames Laboratory Coal Laibrary. Prior to use, the coal was ground, sized, dried at 110 °C overnight under vacuum, and stored under a nitrogen atmosphere. The solvents were distilled by ordinary procedures before use. The quantitative determination of the ratio of the concentrations of solvents in the system were carried out by a gaschromatography using a packed column ( $\Phi=1/8'$ , glass columnn, 2m, PDEGS). A typical run was as follows: To Illinois #6 coal (500mg; 60-100mesh), a mixture of triethylamine and methanol (1.5ml; 1:2 vol.) was added, and immersed in the ultrasonic cleaning bath. An aliquot of the supernatant of the mixture was injected into a gaschromatography with appropriate time intervals.

## RESULTS AND DISCUSSION

### Swelling of Illinois #6 Coal in Binary Solvent System

Figure 1. shows the swelling behavior of Illinois #6 coal in the systems of triethylamine and methanol, and dimethylaniline and methanol.

As Hombach already reported(4), in these case also significant synergistic effects were observed. However, curiously enough such effects did not appeared in the systems such as pyridine/methanol or n-propylamine/methanol, in spite of their reasonable ranges of the solubility parameters ,as shown in Figure 2.

Furthermore, in the case of the use of steric isomers of butylamine, n-butylamine and t-butylamine, the synergistic effect was observed only to the sterically hindered isomer system(Figure 3).

Figure 4. shows the solvent swelling behaviors of Illinois #6 coal in the binary solvent systems of which components' solbility parameters are considered to be quite similar, i.e., hexamethylphosphoramide(HMPA) / dimethylformainde (DMF) or t-butylmethylketone(pinacolone) / acetone, in which also sinergistic effects appeared.

These observations clearly suggest that the sinergistic effects of binary solvents on the swelling of coal were not resulted by such simple parameter as a solbility parameter.

Recently, we have revealed the steric requirement on the solvent swelling of coal(6). Based on our observations, such solvents as triethylamine, dimethyl aniline, t-butylamine, pinacolone or HMPA showed significant retardations on

their penetration rates into coal matrix(8). On this point of view, it is quite likely that because of their steric bulkiness, the apparent equilibrium swelling ratios(Q-values) of these solvents are forced to keep far below their potential values expected under more relaxed steric requirement of coal. .

#### Measuring the Relative Concentrations of Binary Solvents During Swelling of Illinois #6 Coal

In order to examine the possibility of the selective penetration of the solvent molecule of the binary system into the coal matrix, the relative concentrations of the solvents in the supernatant of the mixture were determined during swelling the coal.

Figure 5. illustrated the change of the relative concentration of methanol vs. time, together with the swelling behavior of coal.

It is obvious that the penetration of methanol into the coal matrix occurred predominantly, that is, the relative concentration of methanol in the supernatant was sharply decreased at the initial stage of swelling of coal, and then kept almost constant value which was still a little below the original concentration.

Table 1. shows the relative swelling rate (retardation factors;  $V_{rel}$ ) of the various solvents to Illinois #6 coal at 21°C, which were calculated as described into previous report(7). In these data, we can see that the penetration rate of methanol is approximately 10\* times faster than that of triethylamine.

#### Plausible Mechanism of Synergistic Effect of Binary Solvent on Swelling of Coal.

All of these observations described above may be rationalized as follows: The swelling of coal in the binary solvent systems composed of a sterically hindered and a less sterically hindered solvents( or in general, the solvents possessing different penetration rates) is initiated by the predominant penetration of the less hindered solvent, and then forms , so-called, "Coal Gel", of which steric requirement will be released significantly because of the expansion of the coal matrix by the penetrant, and thus it enable to penetrate more sterically hindered solvent molecule into coal with a "Edge Effect".

Namely, the synergistic effect of binary solvent on the swelling of coal is considered to be resulted by the relaxation of the steric requirement of coal, based on the "Coal Gel" formation.

#### ACKNOWLEDGEMENTS

This research was supported by the special grant from The Environmental Science Institute, Kinki University of JAPAN. We are also grateful for support from The State of Iowa, and from the U.S. Department of Energy through the Ames Laboratory under Contract No. W-7405-ENG-82.

#### REFERENCES

1. A. Wielopolski, I. Witt, Koks, Smola, Gaz, 22, 47 (1975)
2. M. Iino, J. Kumagai, O Ito, J. Fuel Soc. Japan (Nenryo Kyokaiishi), 64, 210 (1985); Proceedings of 2nd Japan-China Symposium on Coal & C<sub>1</sub> Chem., Tokyo, Japan, 309 (1988)
3. I.G.C. Dryden, Fuel, 30, 39, 145, 217 (1951); D. W. van Krevelen, "Coal", Elsevier Publishing Co., Amsterdam (1961)
4. H-H. Hombach, Fuel, 59, 465 (1980)
5. J.W. Larsen, T. K. Green, Fuel, 63, 1538 (1984)
6. T. Aida, T. G. Squires, Prepr. Pap.-Am. Chem. Soc., Div. Fuel Chem., 30, 102 (1985)
7. T. Aida, T. G. Squires, Prepr. Pap.-Am. Chem. Soc., Div. Fuel Chem., 30, 95 (1985)
8. T. Aida, K. Fuku, N. Yamawaki, M. Fujii, unpublished results.

Table 1. Comparison of Swelling Rate  
(Illinois #6, 60-100 mesh, 21 °C)

SOLVENTS	$V_{Ret.}^*$
Methanol	1.00
Acetone	0.86
Dimethylformamide	0.24
n-Butylamine	0.10
t-Butylamine	39.75
Dimethylaniline	105.43
Triethylamine	$> 10^4$
Pinacolone	$> 10^9$
Hexamethylphosphoramine	$> 10^4$

\* Retardation Factor =  $V_{MeOH} / V_{Solvent}$

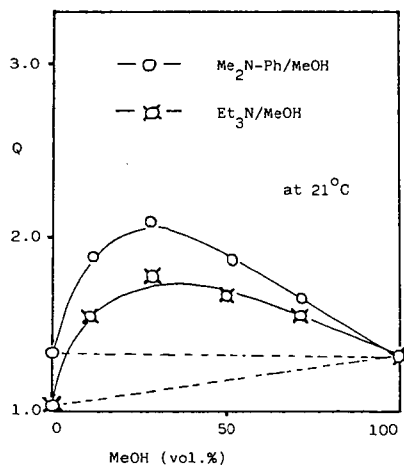


FIGURE 1.

Solvent Swelling of Coal in Binary System  
(Illinois #6 Coal, 60/100 mesh)

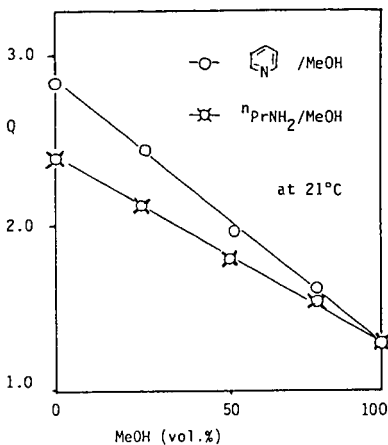


FIGURE 2.

Solvent Swelling of Coal in Binary System  
(Illinois #6 Coal, 60/100 mesh)

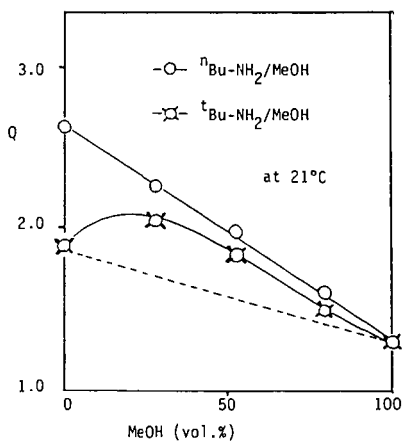


FIGURE 3.

Solvent Swelling of Coal in Binary System  
(Illinois #6 Coal, 60/100 mesh)

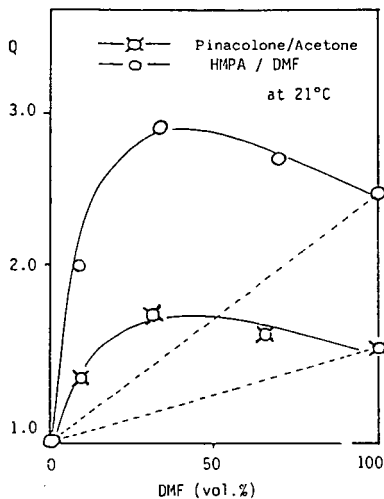


FIGURE 4.

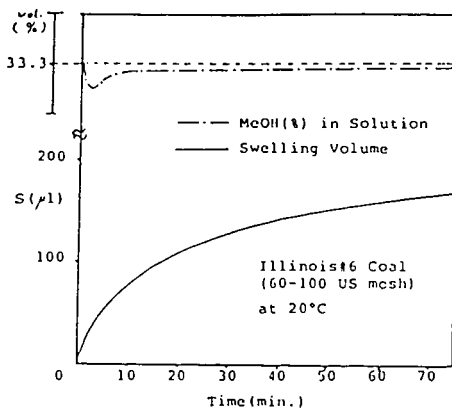


FIGURE 5. Solvent Swelling in Binary Solvent System  
(Et<sub>3</sub>N/MeOH) and Change of Composition  
in Solution

Utility of Low Value Liquefaction Products  
as a High Value Additive

Hyon H. Yoon and Arthur R. Tarrer

Chemical Engineering Department  
Auburn University, AL 36849

Characteristic to many coal liquefaction processes is that certain streams have objectionable properties in terms of ease of upgrading, and as a result, these streams not only complicate downstream processing but have a very low value. A specific objective of this research was to identify a high value application for these streams. This can impact the entire coal liquefaction processing train and its economics. By finding a high value application for these streams, it becomes economical to remove them early in the processing train for separate processing. This simplifies downstream processing of other streams, reducing overall processing costs, with there being an actual higher value for the entire product slate.

Typical objectionable properties of certain coal liquefaction streams are: 1) high molecular weight distribution, 2) high heteroatomic content, and 3) high metals content. (1) It was thought that these objectionable properties could actually prove to be advantageous for utilizing these fractions as a high value antistripping additive for asphaltic pavement cement.

Stripping of asphaltic cement from pavement aggregates has long been recognized as a major cause of failure in asphaltic concrete pavements. The cause of stripping is attributed to water or moisture penetrating the asphalt-aggregate matrix. Stripping, which is the loss of adhesive bond between the asphalt and aggregate surface, results in a loss in integrity of the asphaltic concrete and subsequent failure, requiring early and costly maintenance.

A number of methods have been developed for reducing stripping damage in asphaltic concrete pavements. Of these methods, the addition of a chemical antistripping (AS) additive has become the most widely practiced method for maintaining pavement durability, because of its relatively low cost and ease of implementation. A large number of AS additives, which are normally surfactants, are commercially available today. According to the 1984 survey of state highway agencies by Tunncliffe and Root (2), more than 100 chemical AS additives are used in the United States.

AS additives are substances added to asphalt cement to promote adhesion of the asphalt cement to the aggregate surface and thus to improve the resistance of the asphalt pavement to stripping damage. Most AS additives are mixtures of proprietary chemical compounds, and detailed characterizations of these compound mixtures are usually not available; however, most of the active compounds are probably amines or chemical compounds derived from ammonia. Usually these compounds act as cationic surfactants to reduce surface tension at the aggregate surface (3). However, it has been shown that many AS additives are susceptible to heat and thus, with storage in hot asphalt cement, the effectiveness of these additives could be severely reduced. Figure 1 shows the loss in effectiveness for different typical commercial AS additives with storage of the additives at 325°F in an asphalt cement. Four

different commercial AS additives from different manufacturers were used in this study. The additives were labeled Additive Nos. 1, 2, 3, and 4. The stripping propensity of an asphalt-aggregate mixture was measured in terms of the percentage coverage of aggregate after the boiling water test. If the asphalt separated from the aggregate surface after boiling the asphalt-aggregate mixture in water for 10 minutes, it was said to have stripped, and the asphalt - aggregate bond was concluded to have been weak and to have a high stripping propensity.

In addition to evaluating the heat sensitivity characteristics of AS additives, it was shown that only a small fraction of the AS additive migrates to the aggregate surface and acts to improve the asphalt cement/aggregate bonding: most of the additive remains in the bulk of the asphalt and never comes in contact with the aggregate surface. For this reason, such chemical AS additives not only change the asphalt cement/aggregate bonding, but can also change the properties of the bulk asphaltic cement significantly.

In order to minimize AS additive dosage requirements, direct application of AS additive to the aggregate surface was investigated. Table 1 shows the result of direct application of an AS additive (Additive No. 1) to the aggregate surface. The additive, which is water soluble, was dissolved in water to form treatment solutions having concentrations ranging from 0.05 to 0.5 wt%. Then the aggregate (granite 3/8 in. - No. 4 mesh size) was immersed in the respective solution for 10 minutes. After towel drying and preheating the aggregate at 275°F, the boiling water test was performed. Based on the results given in Table 1, it was calculated that direct application of AS additive to the aggregate surface requires only about 5% of the amount of additive which would be required to provide an equivalent effective amount of additive at the aggregate surface when the additive is added in the asphalt.

With direct application, the commercial AS additive, a polyamine-type additive, appeared to degrade at relatively high temperatures (250°C) and become ineffective, as shown in Figure 2. The preheating temperature was varied from 135°C to 350°C to simulate the temperature range in which aggregates may be heated in a commercial aggregate dryer. The temperature of combustion gases and air used to dry aggregate in a commercial dryer ranges from about 250 to 315°C.

In an earlier work (4), it was found that stripping of asphalt cement from pavement aggregates was very much an aggregate problem. That is, physico-chemical properties of the aggregate surface have a very significant effect on the stripping propensity of an asphalt-aggregate mixture. Figure 3 shows how the surface charge density (Zeta Potential) varied among some different types of common aggregates. Interestingly, the aggregates which had a relatively high surface charge were found to be more susceptible to stripping as measured by the boiling water test.

It was thought that by impregnating the aggregate surface with an easily polymerized compound prior to its being dried, it would become coated with molecular layers of polymerized (coked) material. This could serve to reduce the surface charge of the aggregate surface and make it easier for the asphalt to adsorb (or bond) to the aggregate.

Aggregate surfaces were assumed to interact strongly with high molecular weight, aromatic compounds in a manner similar to how coke forms on catalyst surfaces. High molecular weight aromatic compounds have high coking propensities. For this reason, a granite aggregate was precoated with a phenanthrene solution (10 wt% in toluene) and then preheated at 135, 250, and 350°C. Figure 4 shows that the effectiveness of the phenanthrene pretreatment increased as the preheating temperature was increased. A similar result was obtained for an actual coal liquid (10 wt% toluene), as is shown in Figure 4. The coal liquid was obtained from the Wilsonville coal liquefaction plant. It was therefore thought that the formation of coke-like compounds on the aggregate surface during the aggregate preheating (drying) period could be the primary cause of the observed pretreatment effect of phenanthrene and/or heavy coal liquid on the asphalt-aggregate bond, as was measured here using the boiling water test.

While performing the above aggregate surface conditioning studies, it was observed that reheating an asphalt-aggregate mixture usually resulted in an increase in its stripping resistance. Asphalt-aggregate mixtures were cured (reheated) by holding the mixtures at a fixed temperature for a set period of time. It was observed that the performance of an asphalt-aggregate mixture was improved with curing at about 300°F for several hours. This apparent improvement in adhesion between the asphalt and the aggregate surface with curing was again thought to be, in part, due to coke-like compounds being formed on the aggregate surface. For this reason, pretreatment of a granite aggregate with phenanthrene, which has high coking propensity, was evaluated for accelerating the curing effect on stripping propensity. Indeed, this was found to accelerate curing, as shown in Figure 5.

It appears then that compounds having a high coking propensity, like phenanthrene and heavy coal liquid, have potential usage as an AS additive.

#### References

1. Nalitham, R.V., "Parametric and Kinetic Studies on Deactivation and Regeneration of Hydrotreating Catalysts in Solvent Refined Coal Upgrading Process and an Evaluation of the Liquid Vaporization Effects on Hydrotreater Performance." Dissertation, Auburn University, 1983.
2. Tunnickliff, D.G and R.E. Root, "Use of Antistripping Additives in Asphaltic Concrete Mixture." NCHRP Report 274, 1984.
3. Mathews, D.H., "Surface-Active Agents in Bituminous Road Materials." J. Appl. Chem. 12, February, 1962.
4. Yoon, H.H. and A.R. Tarrer, "Effect of Aggregate Properties on Stripping." Transportation Research Record (In Press).

Table 1. Effect of Aggregate Pretreatment with a Commercial AS Additive (Additive No. 1) on the Boiling Water Test Results.

Additive Content in Water	Water Content of Aggregate after Soaking	Amount of Additive on Aggregate	Percent Coating Retained after Boiling
%	g water/g agg.	g add./g agg.	%
0.5	0.0232	$1.60 \times 10^{-4}$	100
0.1	0.0281	$0.28 \times 10^{-4}$	100
0.05	0.0430	$0.21 \times 10^{-4}$	95
0.05	0.0221	$0.11 \times 10^{-4}$	65
0.05	0.0201	$0.10 \times 10^{-4}$	60

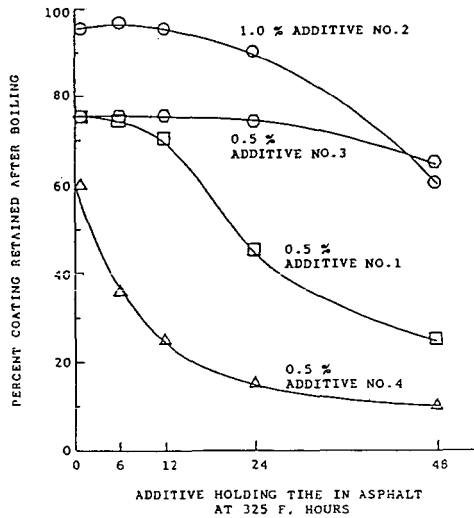


Figure 1. Heat Stability of Antistripping Additives in Asphalt as Determined by the Boiling Water Test.

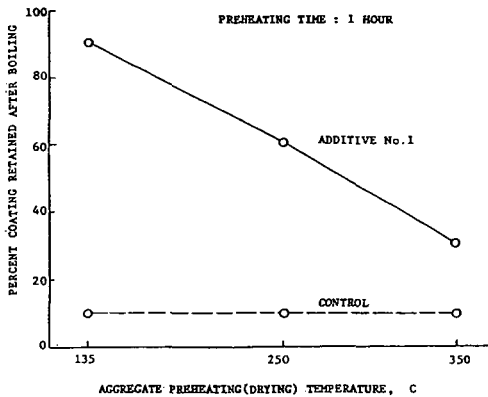


Figure 2. Response in Effectiveness of a Typical Commercial AS Additive to Changes in Aggregate Preheating (Drying) Temperature with Direct Application of the Additive to Granite Aggregate.

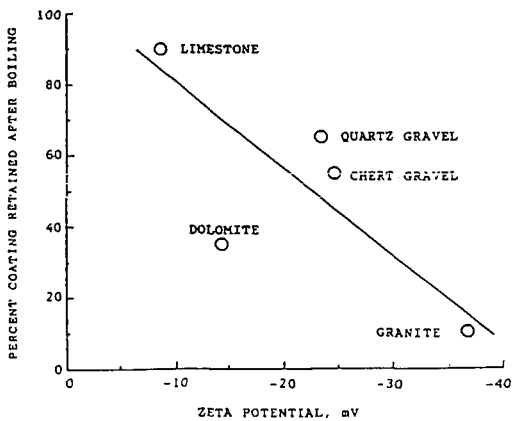


Figure 3. Comparison of Aggregate Surface Potential and Stripping Propensity as Determined by the Boiling Water Test.

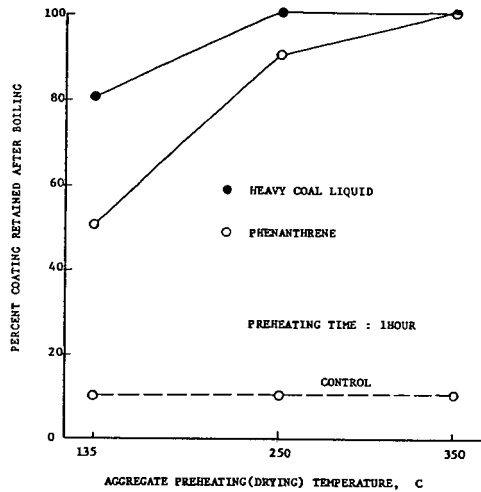


Figure 4. Response in Effectiveness of Phenanthrene and of Coal Liquid as AS Additives to Changes in Aggregate Preheating (Drying) Temperature with Their Direct Application to Granite Aggregate.

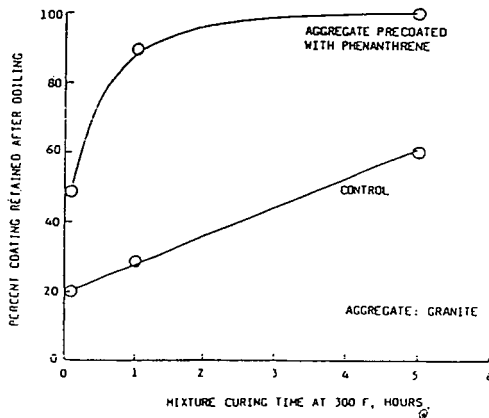


Figure 5. Acceleration of Curing Effect on Stripping Resistance by a High Coking Propensity Additive, Phenanthrene.